

# Investigations on Levee Breach Closure Procedures

M. Hanif Chaudhry  
Mohamed Elkholy  
Cyrus Riahi-Nezhad



Department of Civil and  
Environmental Engineering

300 Main Street  
Columbia, Sc 29208  
(803) 777 3614  
[cee@email.sc.edu](mailto:cee@email.sc.edu)

November 2010

*This research was sponsored by the University of Mississippi/ the Department of Homeland Security. The opinions, findings and conclusions expressed in this report are those of the authors.*

## EXECUTIVE SUMMARY

Hurricane Katrina, category 4 storm, caused many breaches in New Orleans levees; the 17<sup>th</sup> Street Canal levee breach being the most catastrophic. The US Army Corps of Engineers started the closure of the 17<sup>th</sup> Street breach by helicopters to place 3000 Ib sandbags. Later the size of the sandbags was increased to 6000 and 7000 Ibs because the lighter bags were washed away by the flow through the breach. Plans in the field for breach closure were changed a couple of times because of the absence of standard procedures. A 1:50 scale model was constructed in the hydraulic laboratory at the University of South Carolina to simulate the 17<sup>th</sup> Street Canal levee breach and the flooded neighborhood. The physical model has been validated against available data in the IPET (2007), where the measured maximum breach discharge was 31,699 cfs as compared to about 29,000 cfs as calculated in the IPET (2007). The measured flooding depths in the vicinity of the breach ranged from 4 ft to 6 ft and then decreased to an average value of 2.2 ft at about 400 ft from the breach, which are very close to high water marks of elevations 2.3 ft to 2.8 ft collected at 400 ft from the breach and the scaled video recording of 4-5 ft near the breach (IPET 2007).

Tests showed that, with water elevation in the channel of 9 ft, the 6,000 Ib sandbags used by the USACE would be easily washed away and that sandbags weighing 30,000 and 50,000 Ib would be required to close the breach. Tests show that the 17<sup>th</sup> Street canal breach could have been closed using lighter sandbags by utilizing various closure procedures for cofferdam closure, e.g., transverse dumping, toe dumping and multi-dike system. The proposed research involves the development of digital Particle Tracking Velocimetry Technique for application to particle tracking for breach closure, development of flow velocity versus particle size relationships, different breach closure procedures and velocity profiles in the physical model for different flow rates.

## TABLE OF CONTENTS

Executive Summary.....	ii
Table of Contents.....	iii
List of Figures.....	v
List of Tables.....	vii
Chapter 1.....	1
Introduction.....	1
Background.....	1
Objectives.....	2
Experimental setup.....	2
Hydraulic characteristic of the levee breach.....	5
Chapter 2.....	
Tracking Sandbags by Digital Particle Tracking Velocimetry Technique.....	7
Stereoscopic configurations.....	8
Translation system.....	8
Results.....	11
Chapter 3.....	
Threshold of Sandbag Motion.....	16
Experimental setup.....	17
Volume of sandbags.....	18
Experimental procedures.....	18
Analysis of experimental results.....	20
Critical velocity of sandbags.....	20
Critical shear stress.....	21
Chapter 4.....	
Stability of Sandbags.....	23
Breach closure.....	24
Multi-Barrier Type 1 (MBT1).....	25
Multi-Barrier Type 2 (MBT2).....	26

Single-Barrier embankment.....	26
Closure of Canal at Old Hammond Highway Bridge.....	28
Discussion.....	29
Chapter 5	
Velocity Profiles in Katrina Model.....	31
Results.....	33
Summary and Conclusions.....	38
References.....	39

## LIST OF FIGURES

Fig. 1.1	Schematic description of the physical model setup	3
Fig. 1.2	Katrina model	4
Fig. 1.3	The scour hole caused by landing slide and flood flow	6
Fig. 2.1	Translation system	9
Fig. 2.2	The high speed camera and the lens used for tracking the sandbags	10
Fig. 2.3	Model sandbags starting from the left by 4,000 – 7,000 – 10,000 – 15,000 and 30,000 Ibs.	10
Fig. 2.4	Particle tracking (a) before segmentation, (b) after segmentation and locating the centroid of the particle	11
Fig. 2.5	Image pairs of 44.4 KN (10,000 Ib) sandbag	11
Fig. 2.6	Contour map for the dry bed elevation in the model	12
Fig. 2.7	Trajectories of 10,000 Ib sandbag at five locations along the breach	13
Fig. 2.8a	Trajectories of 10,000 Ib sandbag at location 1 for repeated runs	14
Fig. 2.8b	Trajectories of 10,000 Ib sandbag at location 3 for repeated runs	14
Fig. 2.9a	Trajectories of the 10,000 Ib sandbag in z-direction at locations 1	15
Fig. 2.9b	Trajectories of the 10,000 Ib sandbag in z-direction at locations 3	15
Fig. 3.1	Visual technique method for measuring the volume	19
Fig. 3.2	Critical velocity of sandbag	21
Fig. 3.3	$\tau_*$ versus $R_*$ for sandbags over smooth fixed bed	22
Fig. 4.1	Closure sequence in multi-barrier systems: (a) water flowing with high velocity and momentum through the breach area; (b) sandbag barrier across the breach to reduce flow velocity; and (c) smaller size sandbags can be used to finally close the breach.	24
Fig. 4.2	Toe dumping for Multi-Barrier Type 1 (MBT1)	25
Fig. 4.3	Three- barrier embankment for Multi-Barrier Type 2 (MBT2)	26
Fig. 4.4	Single-barrier embankment. (a) Downstream of the breach with gravel filling the scour hole. (b) Toe dumping for 7,000 Ib sandbag starting from the embankment. (c) Complete closure of the downstream half of the breach	27
Fig. 4.5	Toe dumping of 7,000 Ib sandbag starting from the embankment	28
Fig. 4.6	Closure at Hammond Highway Bridge by using a combination of toe and transverse dumping for Cases 1 and 2 (looking south)	29
Fig. 5.1	A movable grid covering the left side of Katrina model	31

Fig. 5.2	Notations for all the grid points in the model	32
Fig. 5.3	Elevation of flow depths for a flow of 900 gpm in the model	33
Fig. 5.4a	Velocity profiles for 900 gpm at x0 - y3 to y6	34
Fig. 5.4b	Velocity profiles for 900 gpm at x10 - y3 to y6	34
Fig. 5.4c	Velocity profiles for 900 gpm at x24 - y2 to y12	34
Fig. 5.4d	Velocity profiles for 900 gpm at x24 - y13 to y17	35
Fig. 5.4e	Velocity profiles for 900 gpm at x35 - y2 to y7	35
Fig. 5.5a	Velocity profiles for 1500 gpm at x0 - y3 to y6	36
Fig. 5.5b	Velocity profiles for 1500 gpm at x10 - y3 to y6	36
Fig. 5.5c	Velocity profiles for 1500 gpm at x24 - y2 to y5	36
Fig. 5.5d	Velocity profiles for 1500 gpm at x24 - y11 to y15	37
Fig. 5.5e	Velocity profiles for 1500 gpm at x35 - y2 to y6	37

## LIST OF TABLES

Table 3.1	Particle characteristics	19
Table 4.1	Three cases for the stability of sandbags at different locations along the breach	23
Table 4.2	Required sizes of sandbags along the breach for Multi-barrier Type 1 (MBT1)	25
Table 4.3	Number and weights of sandbags used for closure at breach and at bridge	30

# Chapter 1

## Introduction

Flooding has been an important issue since the early settlement of New Orleans since the city is under the sea level. Several levees were breached following hurricane Katrina in August 2005, which is categorized as category 4 storm, inundating most of the city of New Orleans. The 17<sup>th</sup> street breach was the most catastrophic because of the topography of the surrounding area. This breach was approximately 305 m (1000 ft) from Old Hammond Highway Bridge with a breach width of 137 m (450 ft). The US Army Corps of Engineers (USACE) worked around the clock to close the breaches by placing sandbags in the breach. They started with 3,000 lb sandbags and later increased the size of the sandbags to 6,000 and 7,000 lbs because the lighter bags were washed away by the flow through the breach. Plans set in the field for breach closure were changed several times because of the absence of systematic optimum procedures that could be followed. Water through the breaches flooded the city killing people, destroying the infrastructure and tripping pump stations (e.g. pump stations number 6 and 10). Consequently, trial-and-error procedures were employed and it took several days to close the major levee breaches, most of the city was inundated and dewatering activities were substantially delayed. The current research on levee closure is limited and the laboratory investigations for previous studies have been based on the visual observations of the dumped material. Presently, advanced Digital Particle Tracking Velocimetry (DPTV) techniques are available which will allow understanding the mechanics of motion of the sandbags. The findings of the proposed project will facilitate future research to develop systematic optimum procedures for the closure of levee breaches.

## Background

To our knowledge, limited systematic research is available on the closure of a breached levee and thus trial-and-error procedures have been used in the past as was the case in New Orleans. Flooding due to a levee breach has been simulated by several researchers, e.g. Goldman (1997), Gui et al. (1998), Jaffe and Sanders (2001), Ying et al. (2003), and Xu et al. (2005), but the research on how to close a breach is limited. As compared to this, several procedures developed for the closure of rivers by cofferdams and actual data on real-life projects are available, such as

Itaipu Dam in Brazil (Cortim et al. 1977), Cabora Bassa Dam in Isibon (Abacasis et al. 1973), Mangla Dam in Pakistan (Thomas and Gwyther 1967), and Mica Dam in British Columbia (Parmley 1978). Cofferdams are structures that seal off the river temporarily to dry out the areas for the construction of dams, powerhouses, water intakes or navigation locks. Different methods were used to construct the cofferdams, such as transverse dumping, toe dumping, and a combination of both. Most of the ongoing studies and investigations by the governments and other agencies have focused on the reasons for the failure of the levees and how this may be avoided in the future. However, systematic procedures for the closure of the breach and related developments are needed to prepare contingency plans for closing the breached levee in a short time to reduce inundation. This is the primary objective of the proposed investigations.

### **Objectives**

1. Development of digital particle tracking Velocimetry technique for application to particle tracking for breach closure.
2. Development of flow velocity versus particle size relationships.
3. Different breach closure procedures (Toe dumping, transverse dumping and a combination of both).
4. Velocity profiles in a breached levee.

### **Experimental Set-up**

Brief information on the model set-up taken from Sattar, et al. (2008) is included here; for additional details, see this paper.

A schematic of the 1:50 scale physical model used to simulate the 17<sup>th</sup> street canal levee breach and the flooded neighborhood is shown in Fig. 1.1. The model is built in the hydraulic laboratory of the Department of Civil and Environmental Engineering, the University of South Carolina. Data used to build the model are taken from the final report of IPET (2007).

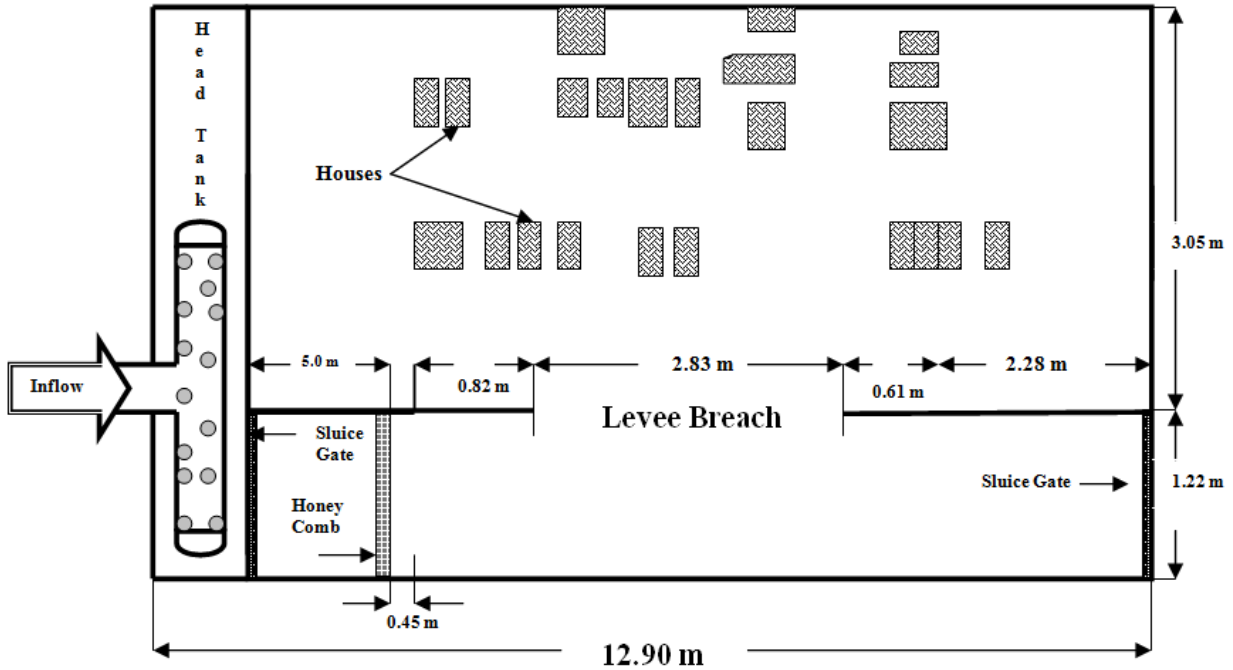


**Fig. 1.1** Schematic description of the physical model setup

An undistorted 1:50 model scale is used to simulate the levee breach. Model-prototype relations are derived based on Froude similitude relationships. The geometric scale of 1:50 was chosen to minimize the effects of viscosity and surface tension in the model. These scale effects are minimized or even eliminated in the scale models of open channels for a geometric scale of 1:50 or 1:25 (Chanson 1999). Moreover, the scale effects may be further minimized by having turbulent flow in the model with Reynolds number for the model, (Chanson 1999). For a water elevation of 0.05 m in the model at the breach location, the flow area,  $A = 0.1382 \text{ m}^2$ , the model wetted perimeter,  $P = 2.586 \text{ m}$ , and the flow,  $Q = 0.0507 \text{ m}^3/\text{s}$ , the Reynolds number of the flow in the model at the breach location is 78,422. For the 7,000 lb and 10,000 lb sandbags, the equivalent diameters on the model are 26.5 and 29.8 mm, respectively. Assuming that the flow around the sandbags has the same velocity as that through the breach the Reynolds numbers for these sandbags are 9,700 and 11,000. According to Henderson (1966), the drag coefficient of the sandbags is more or less constant as long as the Reynolds number is greater than 1,000. Consequently, the results obtained with the model are considered reliable.

The model is constructed in an 11.6 x 6.7 meters (38' x 22') basin. The flooded neighborhood and houses were built on a raised platform to allow outflow in all the three directions to avoid backing up of the water levels, as shown in Fig. 1.2. Two axial pumps each with 0.16 m<sup>3</sup>/s (2500 gpm) are used to supply the flow to the canal during experiments. Discharge is measured by electromagnetic flow meter in the pump delivery line. A screen and a honeycomb are used at the entrance of the canal to reduce turbulence effects and to ensure a smooth water level in the canal. A sluice gate is used to close the downstream end of the canal throughout the experiments where it is assumed that all the breach flow is from Lake Ponchartrain and there is no flow from the upstream pumping stations (this flow was less than 10% of the breach flow for a brief period of time after the canal breach [USACE 2007, p. IV-10-8]).

Since the physical model is to be used to investigate the hydraulics of the 17<sup>th</sup> Street Canal breach and its impact on the surrounding area with various breach closure procedures, the bathymetry and topography of the breach area have to be accurately represented. Therefore, a transverse multi-beam sonar survey for the canal bottom and the breach conducted on the 30<sup>th</sup> of August before emergency closure of the breach (IPET 2007) is used to reproduce accurate details of the topography of the breach area in the physical model.



**Fig. 1.2.** Katrina model (arrows show water flow through the breach and outside the modeled neighborhood)

According to the survey and physical model, the crest elevation of the breach has an average zero meters (0 feet) while the flood walls had an average elevation of 3.65 m (12 ft) throughout the modeled canal section [The USACE 2007 reports mean flood wall elevation of 3.75 m (12.3 ft) on p. II-36-1]. Digital photographs and maps have been used to determine the exact location and dimensions of the houses in the vicinity of the breach, as shown in Fig. 1.2. The physical model represents a 570 m (1,870 ft) section of the 17<sup>th</sup> Street Canal south of the Old Hammond Bridge where the breach occurred and a small part of the neighborhood, 3.172 hectares (7.84 acres) in the vicinity of the breach where major flooding occurred initially and a few recorded high water levels. The Old Hammond Bridge is accurately modeled and the exact dimensions and elevations of all of its components (deck, piles, and pile caps) are obtained from detailed drawings found in the IPET (2007). These detailed drawings are not included in the IPET, but on the USACE website, [www.ipet.wes.army.mil](http://www.ipet.wes.army.mil), in pre-Katrina links. The change in the channel section at the bridge location is also included accurately in the model.

The model is constructed of sealed plywood. The plywood sheets of the channel and the neighborhood area are covered with two layers of thick plastic (3 mm) to ensure waterproofing followed by one layer of metallic chicken wire for strong bonding of the mixture used to construct the topography of the model. The non-erodible topography of the canal, breach and the flooded area were reproduced using a mixture of cement, sand, and zonolite. Irregular topography of the breach and the area at its vicinity are reproduced using plywood frames cut at the exact dimensions of the sections obtained from the IPET (2007) and moved over the specified section in the wet mixture.

### **Hydraulic Characteristic of the Levee Breach**

The breached section of the levee acts as a weir laterally placed across the channel. The weir has an irregular shape with variable crest elevation, length, and slope as shown in Fig. 1.3.



**Fig. 1.3.** The scour hole caused by landing slide and flood flow

The estimated water levels within the 17<sup>th</sup> Street Canal are about 1 m (3 ft) lower than those at the entrance to the canal after the breach was fully formed which is estimated to be 3.65 m (12 ft). Therefore, the water elevation near the breach location was varied from a minimum of 1.22 m (4 ft) to a maximum of 2.74 m (9 ft). In this report, all the flow variables are scaled up to represent the prototype. The breach had a maximum discharge of 898 m<sup>3</sup>/s (31,699 cfs), corresponding to a channel water elevation of 2.74 m (9 ft), whereas a discharge of 352 m<sup>3</sup>/s (12,433 cfs) corresponded to a water elevation of 1.22 m (4 ft). An empirical relationship,  $Q_{breach} = 1.5 H_{canal}^{3.5}$ , fits the experimental discharge-elevation data, where  $H_{canal}$  is the water elevation in the canal upstream of the breach in meters; and  $Q_{breach}$  is the breach discharge in m<sup>3</sup>/s.

The report is divided into five chapters. The Digital Particle Tracking Velocimetry (DPTV) technique to track the motion of the sandbags and to determine the three-dimensional components of the velocity of the dumped sandbags are outlined in Chapter 2. The threshold of motion of the sandbags is discussed in Chapter 3 and the graphical presentation of the critical velocity, critical shear stress and critical Reynolds number of the particle are introduced. In Chapter 4, studies are reported on the stability of the sandbags along a breached levee, and the procedures for the closure of the levee breach efficiently. In Chapter 5, the velocity profiles upstream and downstream of a breached levee for different flow rates are presented. The report concludes with Summary and Conclusions.

## Chapter 2

### Tracking Sandbags by Digital Particle Tracking Velocimetry Technique

In this chapter the use of digital particle tracking velocimetry (DPTV) technique to study the motion of a sandbag during the closure of a levee breach is discussed. This chapter is part of the work reported by El-Kholy and Chaudhry (2009).

Nowadays the particle image velocimetry (PIV) and particle tracking velocimetry (PTV) techniques are utilized successfully. The background literature on PTV is extensive; a recent review article by Adrian (1991) is an excellent starting point for the history of the technique and provides a summary of its development. The basic idea of particle-tracking velocimetry (PTV) is to identify the images of a single particle within an image, segment them from the background, and track them along their trajectories throughout an image sequence. The determination of the particle velocity involves the measurement of particle displacement over a known time interval, defined as  $\Delta s$ , where  $\Delta s$  is the displacement determined by the movement of a studied particle during time interval  $\Delta t$  and  $V$  is the velocity of the particle. During a known time interval, the velocity may be computed by accurately determining the particle displacement  $\Delta s$ , and thus developing the trajectory of the particle.

Many of the PTV methods are restricted to 2D velocity measurements by using a single camera which provides only in-plane velocity components. The information for the out-of-plane flow motion is embedded in the in-plane flow data and the out-of-plane velocity component becomes a source of error in the 2D measurements. However recent 3D approaches using two or more CCD cameras allow on-line data processing to track the particle movement.

Three-dimensional systems based on the methods of digital photogrammetry and the recording of particle image sequences by three synchronized CCD cameras have been developed by Maas et al. (1993). He applied the technique to the measure velocity fields using a number of different test volumes and particle concentrations. Hassan (2001) developed a hybrid system of the stereoscopic, particle tracking velocimetry (PTV) and the shadow image velocimetry (SIV) techniques to provide the shape and trajectory of a single air bubble rising in stagnant water.

In the following sections, the measurements, the imaging system used to acquire flow sequences, and to determine the three-dimensional displacements of a particle in flow are discussed and the results are presented.

### **Stereoscopic Configurations**

Common stereoscopic systems may be classified as (i) translation or lateral displacement systems, and (ii) rotational or angular displacement systems. In the translation system, the axes of both cameras are placed parallel to each other such that they are both orthogonal to the flow. In the angular approach, the optical axes of recording cameras are not perpendicular to the flow but make a certain angle.

3-D velocity vectors are obtained by mapping the displacement from each image plane to the object plane and combining them to obtain the third velocity component. In this study, the translational system is used.

### **Translation System**

The theory of the translation system was described by Arroyo and Greated (1991), and was used by Prasad and Adrian (1993a), Soloff et al. (1997), and Lecerf et al. (1999). The primary advantage of the translation system is its simplicity. Because the object plane, lens plane, and the image plane are all parallel to each other, the image field has uniform magnification. One limitation of the translation system is that there is an upper bound to the off-axis angle  $\theta$  subtended by the center of the region of interest to the center of the lens. This restriction arises purely from the design of the lens since the lens performance degrades as it is forced to operate at the outer limit of its specification. Results obtained by Prasad and Adrian (1993a), Soloff et al. (1997) indicate that the out-of-plane error exceeds the in-plane error by a factor of 3 to 4 for typical installation systems, corresponding to a half angle,  $\theta \cong 15^\circ$ .

The geometric relationship between the true particle displacements ( $dx, dy, dz$ ), and the apparent displacements measured by camera no. 1 ( $\Delta x_1, \Delta y_1$ ) and camera no. 2 ( $\Delta x_2, \Delta y_2$ ), may be derived by examining Fig. 2.1 as

$$\frac{\Delta x_1}{\Delta x_2} = \frac{\Delta y_1}{\Delta y_2} \tag{2.1}$$

$$\text{---} \quad \text{---} \quad (2.2)$$

$$\text{---} \quad \text{---} \quad (2.3)$$

Two high-speed CCD cameras with a resolution of  $640 \times 480$  at 200 frames/second with 256 gray levels are used to track the motion of the sandbags from above. The set-up of the cameras was built to ensure that both cameras can cover the entire area of the levee breach. Fig. 2.2 shows the high speed camera and the lens used for tracking the motion of the sandbags. The height of the cameras can be adjusted from 1.0 m to 3.0 m above the bed of the model.

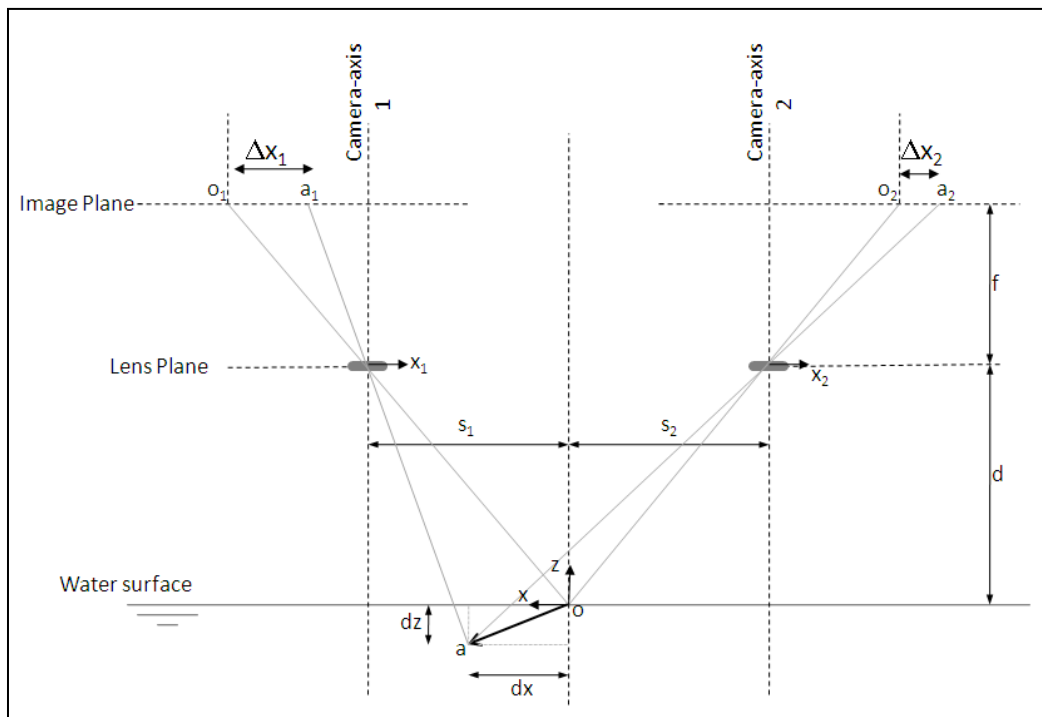


**Fig. 2.1.** Translation system

The distance between the two cameras can be adjusted also every 5.0 cm, up to 50.0 cm. The pictures taken from the camera at an elevation of 1.0 m from the bed covers an area of  $370 \times 270 \text{ mm}^2$ .



**Fig. 2.2.** The high speed camera and the lens used for tracking the sandbags

The bed of the Katrina model in the studied area was painted in a white color. The white color was chosen to improve the images quality. This makes the water look brighter. Besides the sandbags were made of a black cloth to provide good contrast to the bed, as shown in Fig. 2.3. With these colors the extraction of the sandbags from its background and tracking is easier.



**Fig. 2.3.** Model sandbags starting from the left by 4,000 – 7,000 – 10,000 – 15,000 and 30,000 Ibs.

Software was developed to segment the particles from the background and to track them to build their trajectories throughout an image sequence. For the particle segmentation, an interrogation area was chosen 1.2 times bigger than the particle equivalent diameter and the threshold value required to extract the sandbag from the background was chosen from this interrogation area. Based on this threshold value, particle segmentation has to be made for each pixel in the interrogation area to decide whether the pixel belongs to the particle or to the background. Once the particle has been segmented from the background, a sub-pixel accuracy to determine the position of the particle centroid is applied and the coordinates of the particles from each pair of an image is determined. Fig. 2.4 a and b shows an image of sandbag in stationary water, and the same image after extracting the sandbag from the background and locating its centroid.

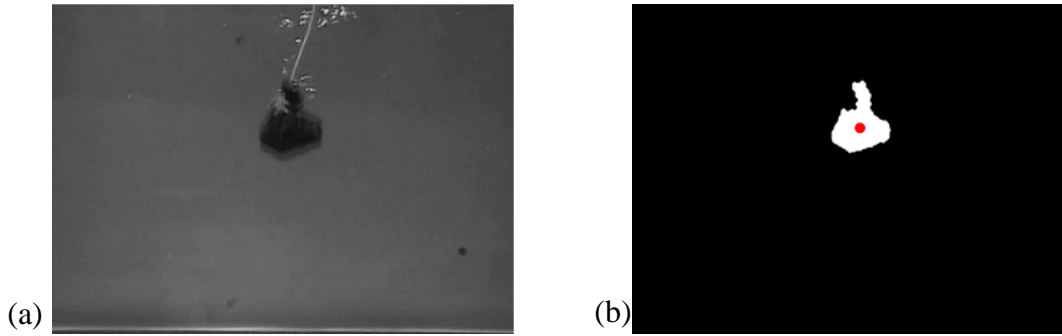


**Fig. 2.4.** Particle tracking (a) before segmentation, (b) after segmentation and locating the centroid of the particle (the centroid appears as small dot)

### Results

In this study, the results are obtained by adjusting the frame rate of both cameras to 100 fps. The distance between the two cameras is 30.0 cm and the vertical distance from the lens plane of the cameras to the top of the levee (the datum in our analysis) is 269.5 cm. These dimensions are chosen to track the dumped sandbags as much as possible and to minimize the error in the out-of-plane trajectory.

An inflow of  $3,350 \text{ m}^3/\text{s}$  is used in this case. The flow was strongly influenced by the topography showing large variation of depth within the model. The average flow depth was about  $18 \pm 2 \text{ cm}$ . A sandbag with a weight of 44.4 kN (10,000 lb) was dropped from just above the water surface to reduce the splashing of the flow surface as the bag hits the water surface. Fig. 2.5 shows a sample of the image pairs taken by the cameras at the same time step for the sandbag. A contour map for the elevation of the dry bed for the studied area is shown in Fig. 2.6. The datum for the elevation of the dry bed is taken as the top of the upstream levee.

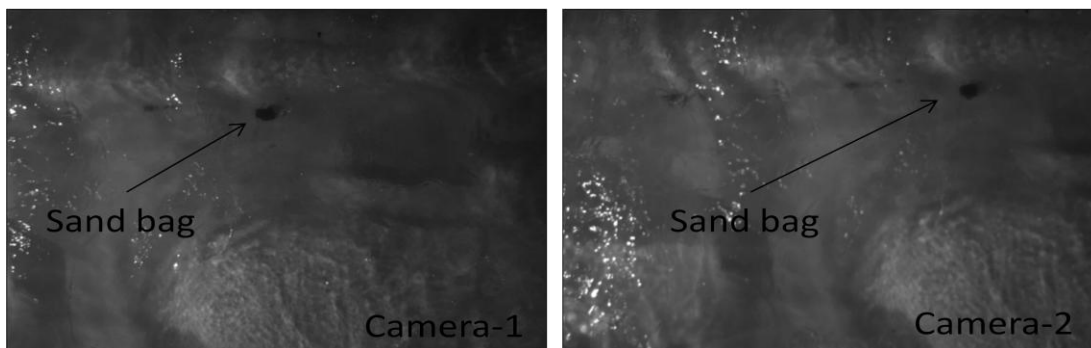


**Fig. 2.5.** Image pairs of 44.4 kN (10,000 lb) sandbag

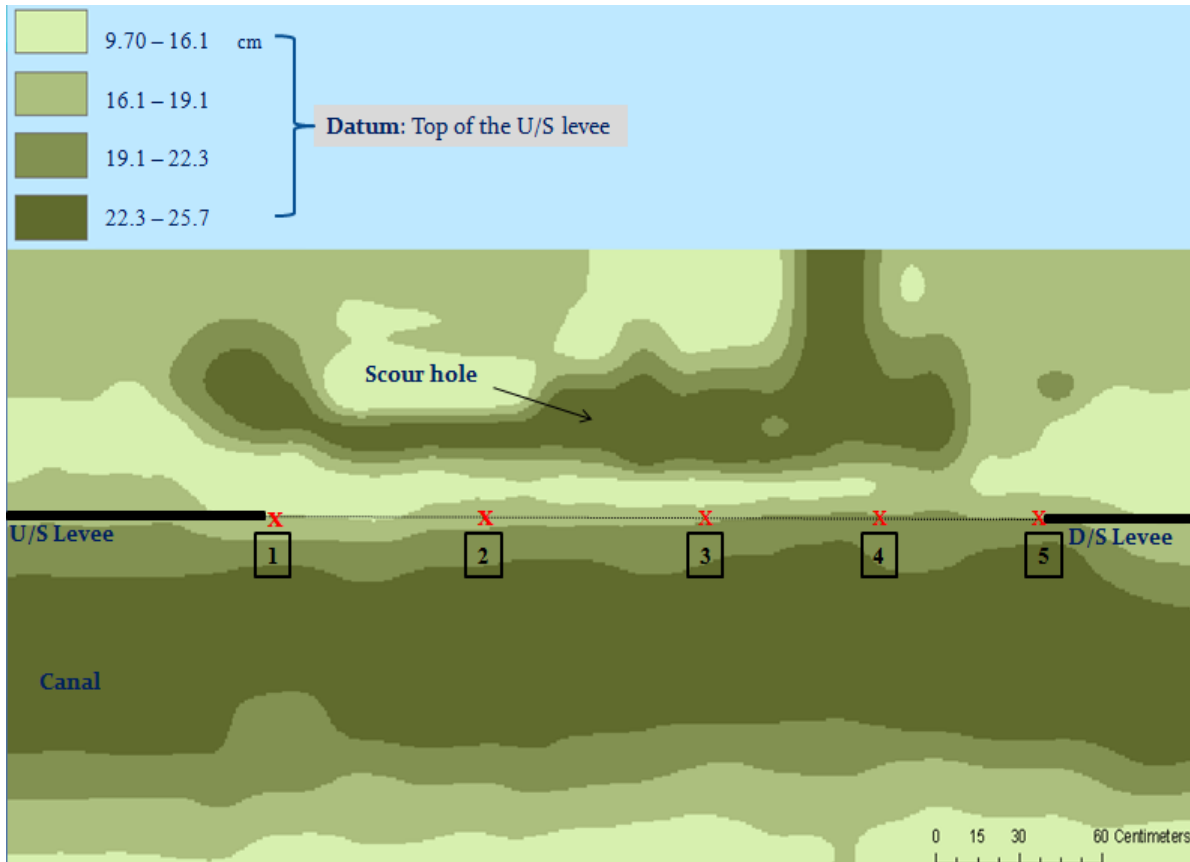


**Fig. 2.6.** Contour map for the dry bed elevation in the model

The dark area in the map represents the lower regions and vice versa. The maximum difference in the bed elevation in the model is 16 cm. The sand bag was dropped at five different locations along the breach, numbered from 1 to 5, with 1 being at the north end of the breach (upstream end) and 5 being on the south end of the breach as shown in the figure. These locations were on the berm of the canal, i.e., on the top of the breached levee section.

At each location, the bag was dropped three times to test for repeatability. Fig. 2.7 shows the trajectories of the sandbags in the plan view for the five locations starting with location 1 at distance  $X = 0.0$  cm and location 5 at distance  $X = 283$  cm. It is clear that the area downstream the breach where the scour hole exists is the controlling area which directs the trajectories of the bags to its exit. It is also shown that the trajectory of the sandbag dropped at location 4 took a long time to exit this area since it was dropped near the area where the flow slows down due to the lower bed elevation in this area. Fig. 2.8 a and b show the repeated runs for the trajectory of the sandbag at location 1 and at location 3 respectively.

The trajectories in the vertical direction (z-direction) were also reproduced, as shown in Fig. 2.9 a and b for the sandbags at locations 1 and at location 3 respectively for three different runs. In the figures, the zero elevation denotes the surface of the water. The results are averaged for every twenty points. All the three runs show consistency in the vertical trajectory. It is clear from the figure that the sandbag for the third run took longer time than the other two runs to travel the same distance. This is because the sandbag may reach a separation zone and then stays there until the drag force pushes it back to move.

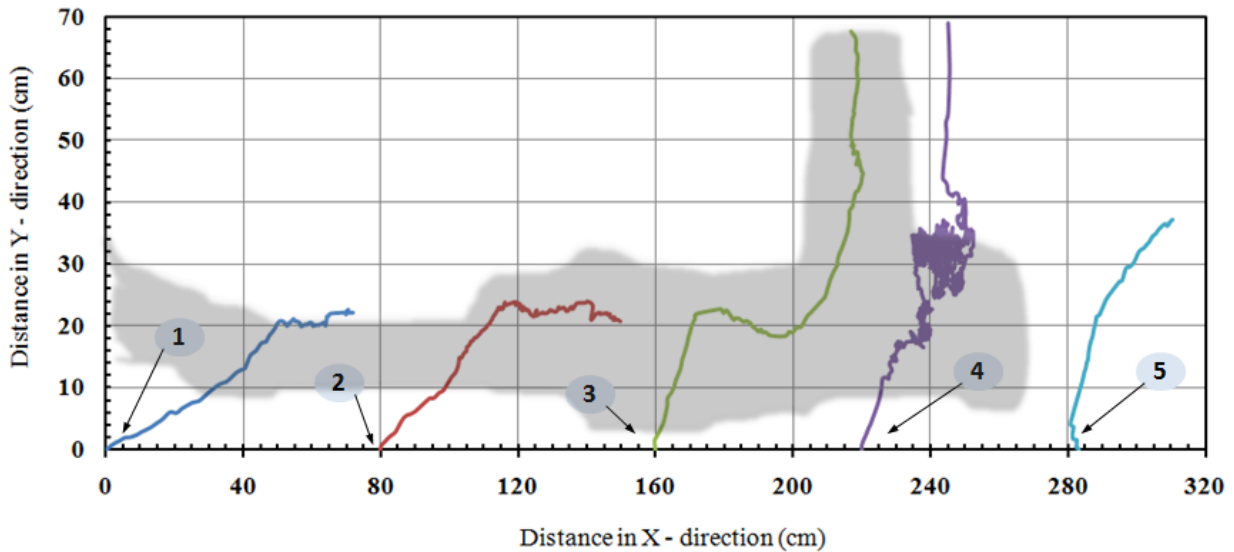


**Fig. 2.7.** Trajectories of 10,000 lb sandbag at five locations along the breach

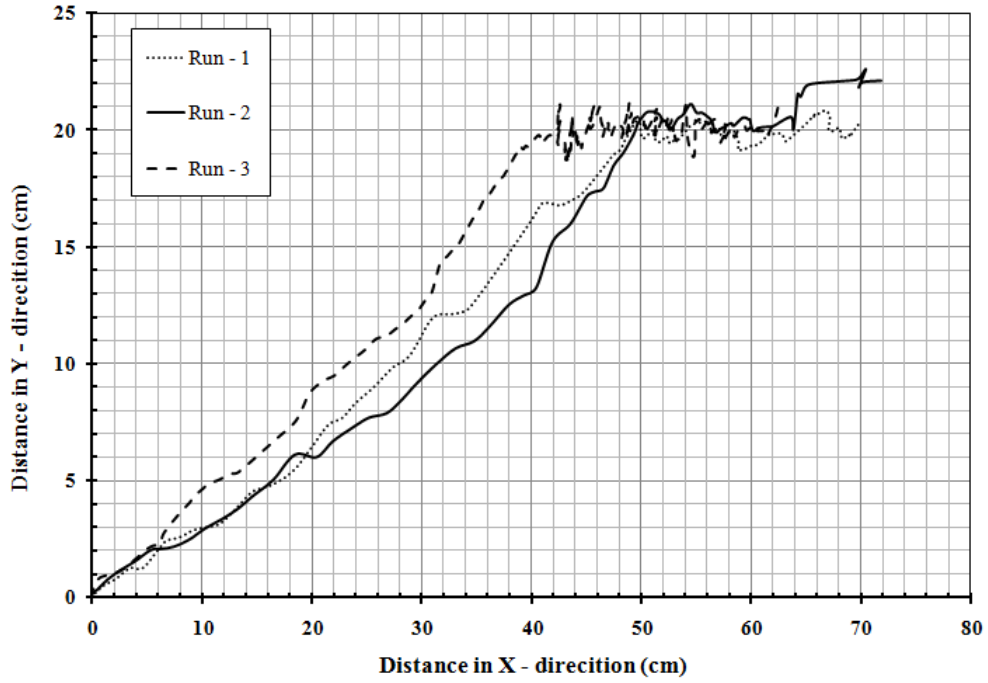


**Fig. 2.8a.** Trajectories of 10,000 lb sandbag at location 1 for repeated runs

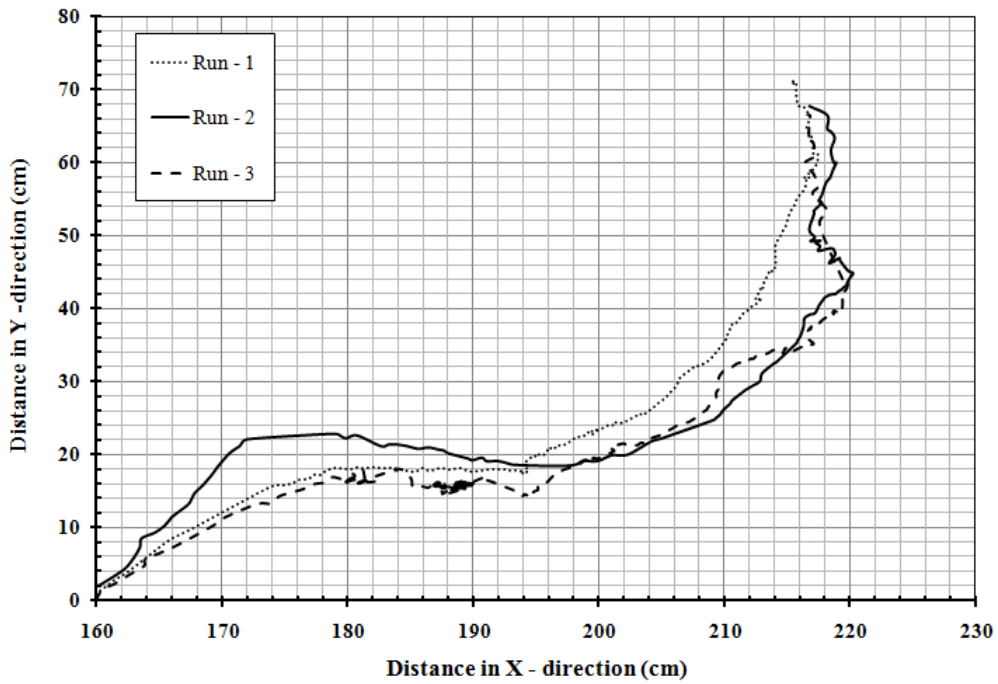


**Fig. 2.8b.** Trajectories of 10,000 lb sandbag at location 3 for repeated runs

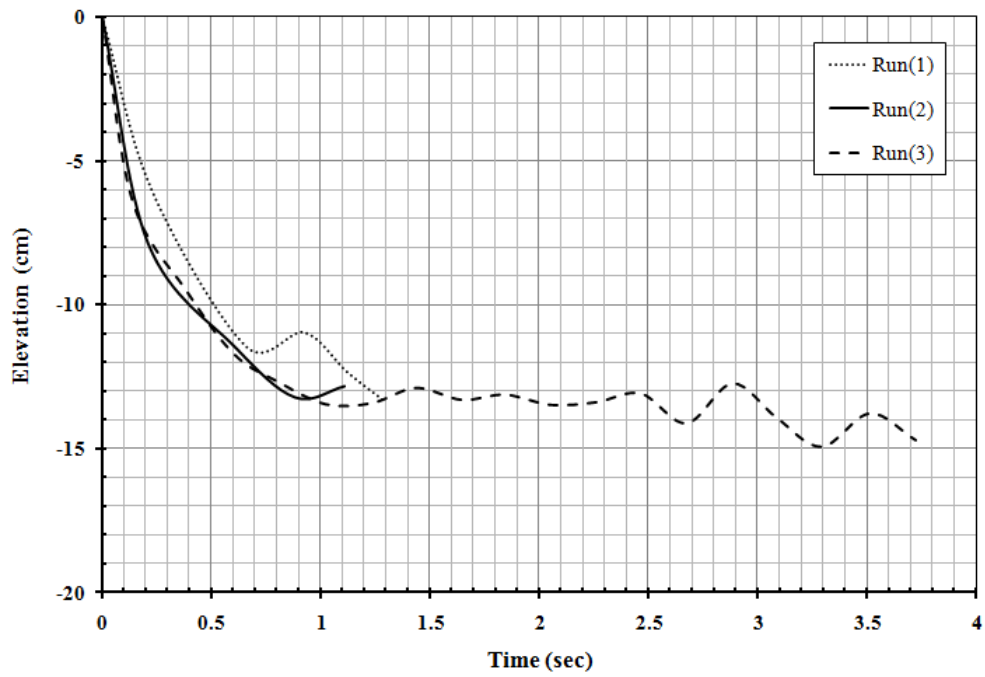


**Fig. 2.9a.** Trajectories of the 10,000 lb sandbag in z-direction at locations 1

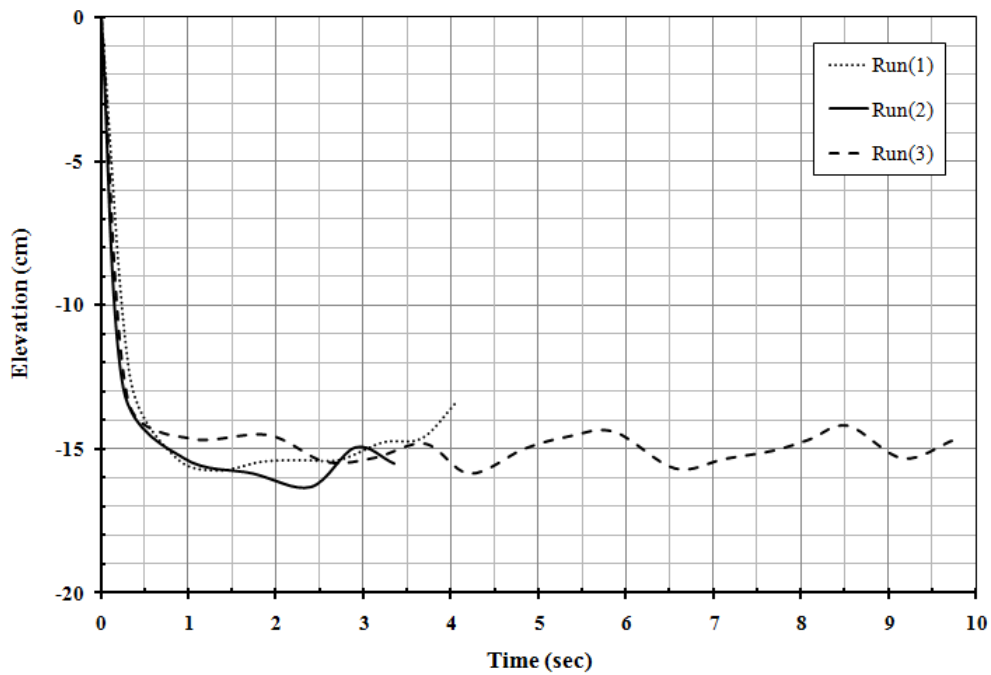


**Fig. 2.9b.** Trajectories of the 10,000 lb sandbag in z-direction at locations 3

## Chapter 3

### Threshold of Sandbag Motion

In this chapter threshold of motion of a single sandbag in open-channel uniform flow is investigated. This chapter is part of the work reported by El-Kholy and Chaudhry (2010). Graphical presentations are included for the critical flow velocity, the critical shear stress, and the critical Reynolds number of the particle for initiating the motion of the sandbag.

The concept of threshold of motion is very important for sediment transport, in theory and in practice. The threshold of sediment is guided by the ratio of the driving forces (drag and lift forces) to the stabilizing forces (submerged weight of the particle). Practically, it is difficult to establish the flow condition where there is no movement of the particle which indicates that the threshold of sediments is a stochastic phenomenon and statistical in nature (Lavelle and Mofjeld (1987)). Shields (1936) investigation on the initiation of motion is the best known and most widely used. He used two dimensionless parameters to determine the initiation of motion of the particles. The first parameter is the dimensionless critical shear stress, where  $\tau_{*c}$  is the critical bed-shear stress,  $g$  is the acceleration due to gravity,  $\gamma_s = \frac{\rho_s - \rho_f}{\rho_f}$  = specific gravity of the particle, where  $\rho_s$  and  $\rho_f$  are the density of the particle and the fluid respectively, and  $d$  is the particle diameter and it represents here the diameter of a volume-equivalent sphere. The second parameter is the Reynolds number of the particle, where  $u_* = \frac{\tau_{*c}}{\rho_f \nu}$  is the shear velocity and  $\nu$  is the kinematic viscosity of the fluid. The American Society of civil Engineers Task Committee on the preparation of a sediment manual (Vanoni (1977)) proposed an alternative parameter through the use of a dimensionless particle diameter defined as

$$\frac{u_* d}{\nu} \quad (3.1)$$

Shields curve has been modified many times since its original publication. The original Shields data showed a considerable scatter and could be interpreted as representing a band rather than a well-defined curve (Buffington (1999)).

Visual method for the definition of threshold of motion can be subjective. Kramer (1935) outlined four different bed motions, namely, no transport, weak transport where individual

particle moves at certain location, medium transport and finally general transport, where particles of all sizes at all points are in motion.

The present study extends the work done by Novak and Nalluri (1984), Defne (2002) and Zhu et al. (2004). Novak and Nalluri analyzed the incipient motion of single particles in a rectangular flume with both fixed smooth bed and fixed rough bed. They used rounded edge particles with an equivalent diameter of 0.6 mm to 50 mm, with an average relative density of 2.56. Gogus and Defne (2005) investigated also the initial motion of single particles with different shapes and sizes under subcritical, uniform flow condition in a rectangular tilting flume. Their experiments are limited since they used an obstructing element with a constant ratio of 1/5 between the height of the element and the height of the particle. Zhu et al. (2004) investigated the horizontal settling distance and the critical flow velocity at incipient motion of sandbag.

In this chapter, the stability of large sandbags typically used for closing levee breaches under different flow conditions is discussed.

### **Experimental Setup**

The experiments described herein were conducted in a 14-m long, 0.5-m wide, and 0.7-m deep recirculating flume with glass walls. A steel mesh at the flume inlet followed by a honeycomb straightens the flow and reduces the turbulence and then a wave suppressor to reduce the water surface disturbances. A tailgate is located at the downstream end of the flume to control the flow to the flume. The pump has discharge capacity of 145 l/s. An electromagnetic flowmeter is installed in the discharge pipeline feeding the flume with an accuracy of 0.5 l/s. A control valve is located at the end of the discharge pipeline just before the entrance of the flume to regulate the flow. The flow depth is measured by a moving point gauge with an accuracy of 0.1 mm. The tested particles were placed at the bottom of the flume with a trash grabber.

The bed of the flume is made of painted plywood which is suitable for smooth-wall experiments with calculated skin friction coefficient,  $C_f$ , of 0.0035 and the roughness height,  $ks$ , of 0.23 mm. The Reynolds numbers for the experiments done on this smooth, fixed bed ranges from  $1.0 \times 10^5$  to  $4.5 \times 10^5$ .

The velocity profiles are measured by a 16-MHz Acoustic Doppler Velocimeter (ADV) system fitted at the mid-section of the flume. ADV is a high precision instrument that measures all the three components of the flow velocity with fluctuations. The accuracy of the measured velocity is 1% of the velocity range. The minimum distance from the boundary is about 5.0 mm. The point with a mean local correlation coefficient between the transmitted and received pulses below 0.70 is ignored which is a required value for reliable flow measurements (SonTek/YSI 2001).

### **Volume of Sandbags**

The volume of the particle is determined by placing the particle on a rotating table and recording the image of the rotating particle. For each image, the boundary of the particle is defined by segmentation. Each half segmented face is allowed to rotate  $360^\circ$  along the particle axis so that half of the segmented face of the particle is a three-dimensional (3-D) shape. The volume of the particle is then calculated by taking the average volume of these 3-D shapes from each image. This method to determine the volume of the particles is easier and more reliable than the well-known displacement method. The success of the displacement method depends on coating the particle with a thin layer of wax without letting the wax penetrate the pores of the particle. This method is unsuitable for the sandbags since the wax may penetrate through it. The volume of the particles is determined by using the visual technique as illustrated in Fig. 3.1.

Six different sizes of sandbags are used. Table 3.1 shows the notation for each particle, the volume, the diameter of a volume-equivalent sphere, the weight of the particle, and the prototype weight it represents at 1:50 scale.

### **Experimental Procedures**

The free-fall orientation of irregular particles is not random over all possible angles since they typically orient themselves to fall with their broadside orientation so that the minimum length is roughly parallel to the fall direction (Loth (2008)). Most likely particles rearrange themselves to this stable orientation.

**Table 3.1.** Particle characteristics

Notation	Volume (cm <sup>3</sup> )	d (mm)	W <sub>m</sub> (gm)	W <sub>p</sub> (lb)
S2	5.4	21	7.3	2,000
S4	11.9	27	14.4	4,000
S7	18.5	33	24.1	7,000
S10	27.3	37	35.5	10,000
S15	38.9	42	53.7	15,000
S30	78.7	54	109.8	30,000

Therefore, the particles were set on the bed of the flume with their broadside orientation to be more stable under the action of the driving forces. Prior to testing a sandbag, it was saturated for at least 24 hours to make sure that the results are repeatable.

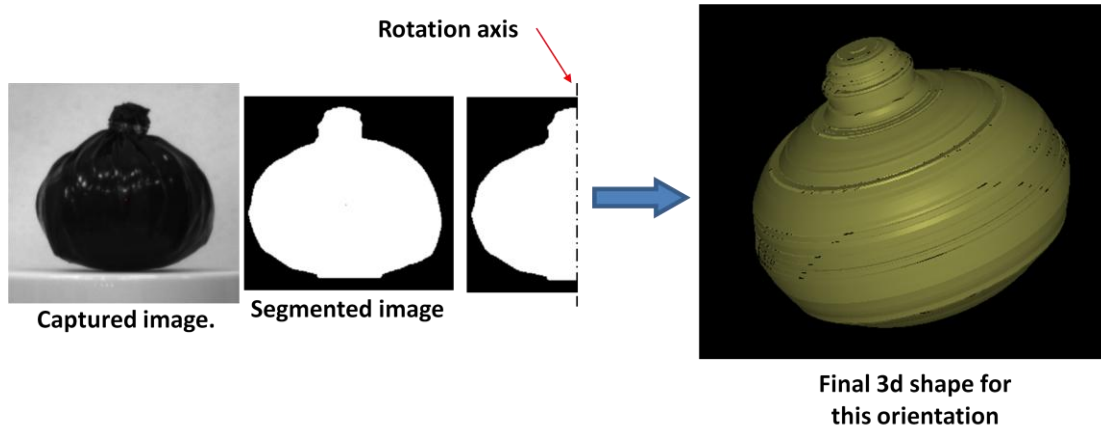


**Fig. 3.1.** Visual technique method for measuring the volume

For each experiment, the downstream gate was first raised to a certain height, the control valve was left in a nearly closed position and the pump was started. The flume was left filled and then the particle was gently placed on the bed along the centerline of the flume with its broadside orientation using a trash grabber. The control valve was then opened gradually in very small

steps to avoid any displacement of the particle while opening the valve. A lag time of 10.0 minutes elapsed between each step so that the flow is steady and for the development of nearly uniform flow condition. The incipient motion is defined here as the start of the sliding of the particle on the bed, or if the particle is about to toss instead of sliding. The criterion for incipient conditions used herein is very well defined and strict. However, scatter is very common with experiments at critical conditions and in sediment transport, in general. In fact, scatter is present in the traditional Shields diagram which is based on the research of several investigators. In this study, major effort was made to minimize the scatter. To reduce some scatter in the result as the experiments are observed by eye which makes it possible to miss some barely detectable particle displacements, the test was repeated at least three times to make the results highly reliable.

## **Analysis of Experimental Results**

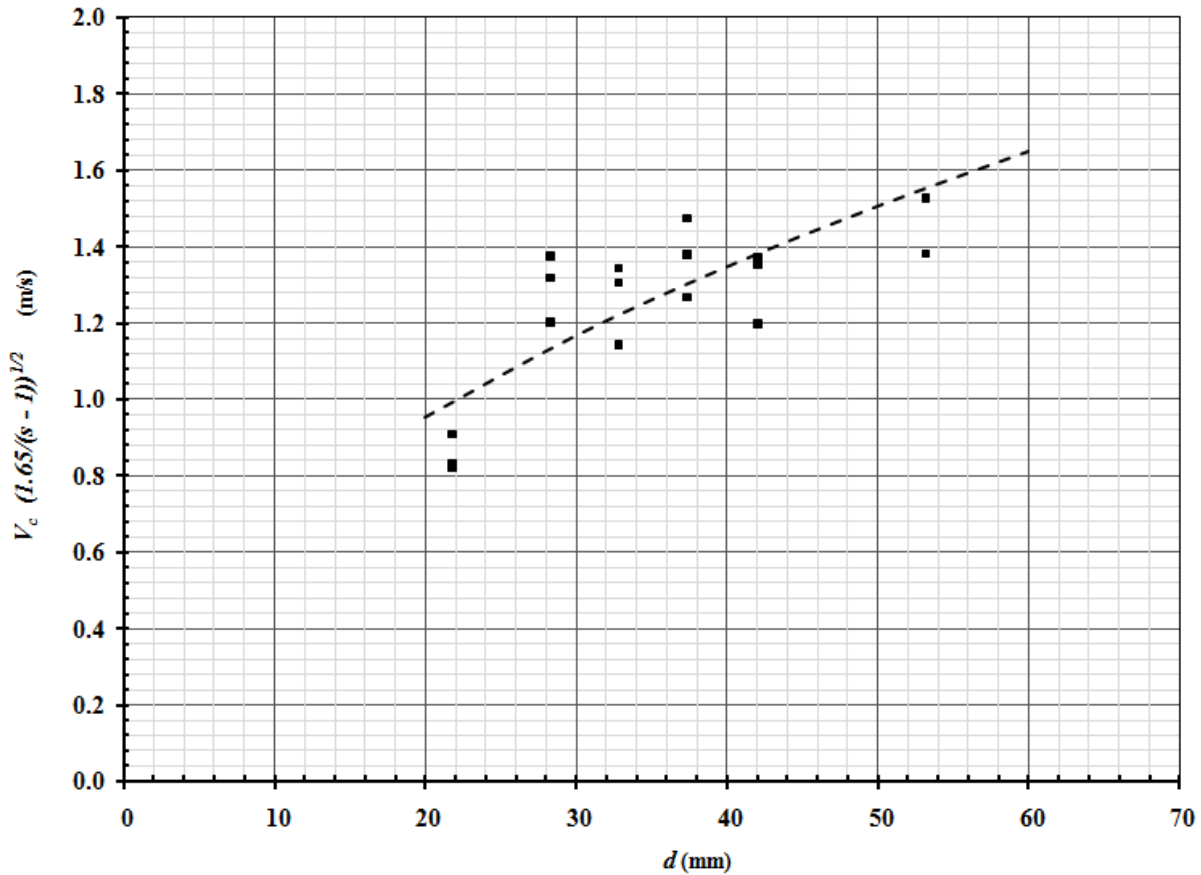
### **Critical Velocity of Sandbags**

Fig. 3.2 shows the relationship between  $V_c$  in m/s and  $d$  in mm for the sandbag-shaped particles, where  $V_c$  is the critical depth-averaged flow velocity required for the initiation of motion of the particle in an open channel with fixed bed. For consistency with material having specific weight of 2.65, the critical velocities have been multiplied by \_\_\_\_\_ . The dry unit weight was used in the analysis. It is clear that larger the particle, higher the flow velocity needed to dislodge it.

Curves were fitted to the results. The fitted equation for the critical velocity of the particle is shown as

$$(3.2)$$

where  $V_c$  is in  $m/s$  and  $d$  is in  $mm$ , and the specific weight,  $s$ , is the dry specific weight of the particle.



**Fig. 3.2.** Critical velocity of sandbag

### Critical Shear Stress

On Shields diagram, the relation between the dimensionless critical shear stress,  $\tau_{*c}$  and the Reynolds number of the particle,  $Re_p$ , for sandbags over smooth fixed bed is shown in Fig. 3.3. From the figure, it can be seen that as the particle diameter increases, its Reynolds number increases, but the dimensionless critical shear stress remains almost within a constant band. This band ranges from 0.003 to 0.008 which is far less than the critical value for the Shields parameter which ranges from 0.03 to 0.08 in the case of alluvial channels. It is noticed also in this figure that each particle experiences different critical shear stress which means that there are other factors affecting the phenomena.

Aguirre-Pe et al. (2003) stated that each particle exhibits a wide range of critical shear stress variation. The general trends for the curves of the sandbag-shaped particles seem to be quite general.

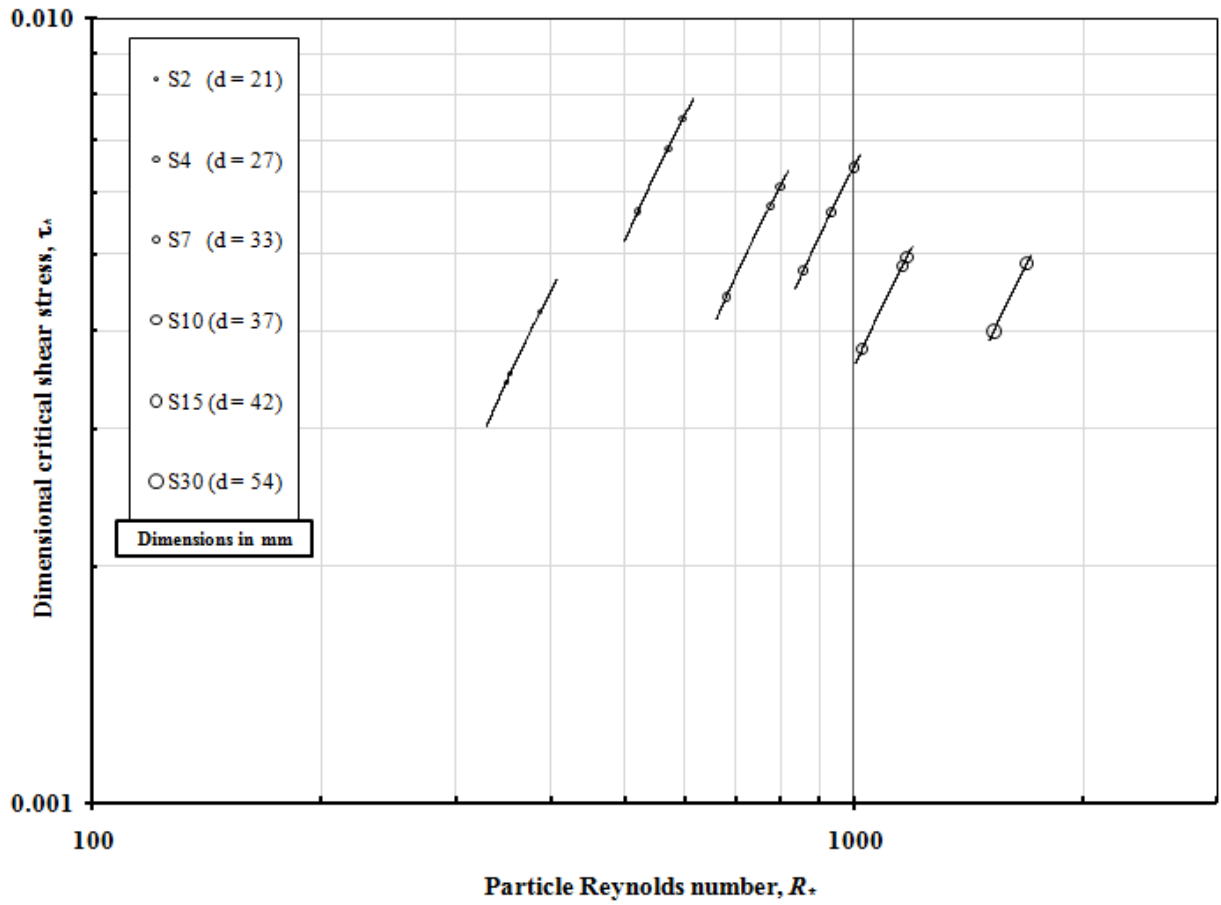


**Fig. 3.3.**  $\tau_*$  versus  $R_*$  for sandbags over smooth fixed bed

## Chapter 4

### Stability of Sandbags

Sandbags are a good choice for closing a breach because of the availability of materials (mostly sand and gravel), the ease of their assembly, and the short time needed to make and drop them to close a breach. Simulations to reproduce the initial failed attempts of the USACE to close the breach of the 17<sup>th</sup> Street Canal by dropping 26.6 kN (6,000 lb) sandbags on August 31<sup>st</sup>, 2005 are discussed in this chapter.

The motion of sandbags of various weights was tested at ten locations along the edge of the breach, equally spaced and numbered from 1 to 10, with 1 being at the north end of the breach near the Old Hammond Highway Bridge and 10 being on the south end of the breach. These locations were on the berm of the canal, i.e., on the top of the breached levee section, as the USACE attempted to close the 17th Street Canal breach in this manner and as the sandbags were unstable in the experiments when they were placed over the sloping side of the channel. Accurate data on the actual failure of the 17th Street Canal flood walls and levees, such as the timing, the progression of the failure, and the degree of blocking of the Old Hammond Highway Bridge by floating debris (USACE 2007, p. IV-10-5), is not available. Therefore, three cases were tested over a range of different variables to obtain a better understanding. The required size of sandbags needed along the breach is summarized in Table 4.1. for the details of these cases, see Sattar et al. (2008).

**Table 4.1.** Three cases for the stability of sandbags at different locations along the breach

Case	Condition	Water elevation (m)	Discharge (m <sup>3</sup> /s)	Required size of sandbags at different locations along the breach
1	Worst	2.74 (9 ft)	898	<ul style="list-style-type: none"><li>• 60% of locations need 50,000 lb.</li><li>• 40% of locations need 30,000 lb.</li></ul>
2	Moderate	1.92 (6.3 ft)	580	<ul style="list-style-type: none"><li>• 40% of locations need 15,000 lb.</li><li>• 20% of locations need 10,000 lb.</li><li>• 40% of locations need 7,000 lb.</li></ul>
3	Mild	1.22 (4 ft)	352	<ul style="list-style-type: none"><li>• 7,000 lb is enough for all locations.</li></ul>

## Breach Closure

In this section, concepts developed for cofferdam closure are utilized, e.g., transverse and toe dumping for the 17<sup>th</sup> Street Canal breach closure by sandbags as the closure materials, and the houses utilized as part of a multi-barrier system. Single and multi-barrier (MB) systems are employed and two types of MB systems are considered. The first type of MB system utilizes two barriers to divide the total head on the breach, thereby reducing the flow velocity through the gap and allows for smaller material to close the breach; this is referred to as MBT1. The second type of MB system utilizes one or more spurs to deflect flows to reduce the flow velocity through the breach which allows for a smaller size of material for closure; this is referred to as MBT2. Schematic representation of the sequence of construction in these two types of closures are shown in Fig. 4.1. Investigations for each of the two MB systems for the first case listed earlier are summarized in the following. The details for the closure procedures of these types of barriers are discussed in Sattar et al. (2008).

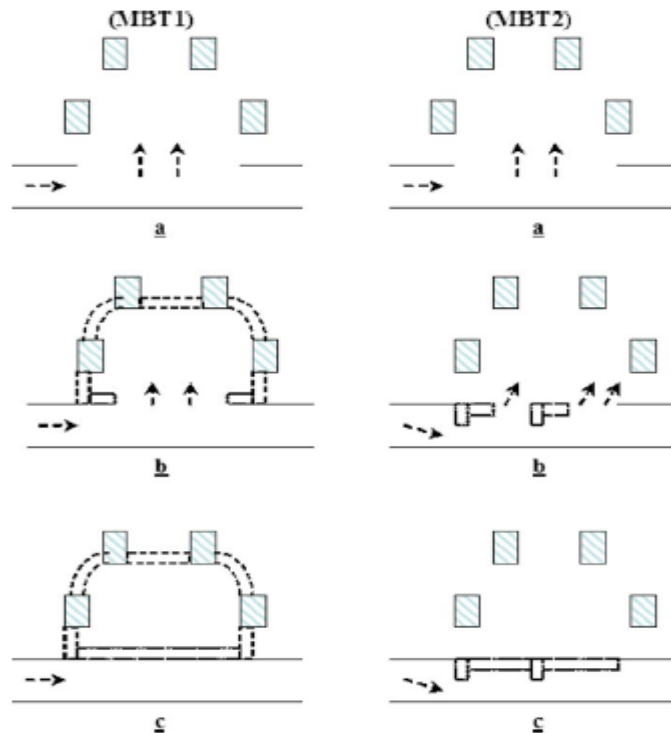


**Fig. 4.1.** Closure sequence in multi-barrier systems: (a) water flowing with high velocity and momentum through the breach area; (b) sandbag barrier across the breach to reduce flow velocity; and (c) smaller size sandbags can be used to finally close the breach.

### Multi-Barrier Type 1 (MBT1)

The force that washes the bags away may be expressed in terms of the differential head between the upstream and the downstream sides of the breach. From the previous geospatial analysis, when the water level is at elevation 2.74 m (9 ft) upstream of the breach, the differential head is 1.67 m (5.5 ft). For breach closure by either transverse or toe dumping, this differential head had to be decreased by raising the water level downstream of the breach by placing 31.1 kN (7,000 lb) sandbags between the houses as shown in Fig. 4.2.



**Fig. 4.2.** Toe dumping for Multi-Barrier Type 1 (MBT1)

Table 4.2 lists the differential head for two trials and the required size of sandbags to close the breach.

**Table 4.2.** Required sizes of sandbags along the breach for Multi-barrier Type 1 (MBT1)

Trial	Differential head (m)	Required size of sandbags along the breach
1	1.14	<ul style="list-style-type: none"><li>• 50% with 7,000 Ib.</li><li>• 50% with 10,000 Ib.</li></ul>
2	0.66	<ul style="list-style-type: none"><li>• Only 7,000 Ib is required.</li></ul>

### **Multi-Barrier Type 2 (MBT2)**

In this type, dumping procedures and barrier construction remained on the channel slopes. Due to high flow velocity in this case, a single barrier embankment was not a good solution for decreasing the flow velocity across the entire length of the breach. Fig. 4.3 shows the three-barrier embankment system. The first and second barriers were constructed by using 133.2 kN (30,000 lb) sandbags and the third was constructed by using 66.6 kN (15,000 lb) sandbags. A 44.4 kN (10,000 lb) sandbag was not washed away on the areas of the breach between the barriers. However, near the south end of the breach, flow was very fast and only a 66.6 kN (15,000 lb) sandbag was not washed away.

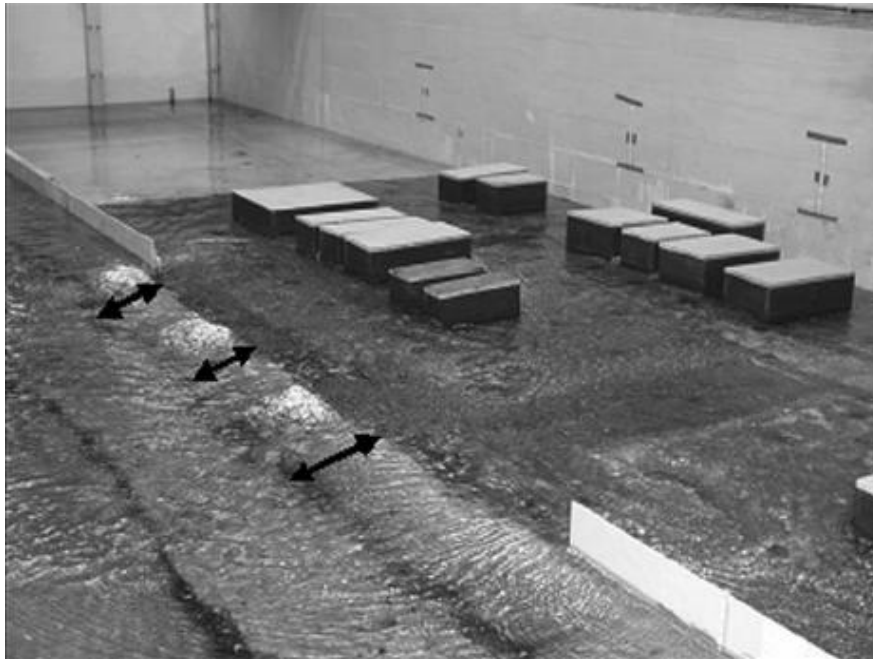


**Fig. 4.3.** Three- barrier embankment for Multi-Barrier Type 2 (MBT2)

### **4.4. Single-Barrier Embankment**

A single-barrier embankment was tested to close the breach for case 2. The barrier was constructed at the middle of the breach. In this case the scour hole was filled with gravel and the gravel was leveled to obtain a flat surface on the side of the houses as shown in Fig. 4.4a.



(a)



(b)



(c)

**Fig. 4.4.** Single-barrier embankment. (a) downstream of the breach with gravel filling the scour hole. (b) toe dumping for 7,000 lb sandbag starting from the embankment. (c) complete closure of the downstream half of the breach

Toe dumping started from the embankment using 31.1 KN (7,000 Ib) sandbags and progressed towards the downstream levee as shown in Fig. 4.4b, and c while the other half of the breach was left open. For this case, the water level in the channel was raised 0.75 m (2.5 ft).

This scenario was repeated again for the closure of the upstream side of the breach while the downstream side was left open. Fig. 4.5 shows the toe dumping starting from the embankment and progressing towards the upstream levee. In this case the water level in the channel was raised 0.65 m (2.1 ft).



**Fig. 4.5.** Toe dumping of 7,000 Ib sandbag starting from the embankment

For these two cases with single-barrier embankment at the middle while the scour hole was leveled, the differential head between the upstream and the downstream side of the breach increased. The increase in the differential head reached almost 40% more than before the closure, which make it difficult to continue closing the open side of the breach.

### **Closure of Canal at Old Hammond Highway Bridge**

The previous sections discussed closure at the breach location; another alternative for the closure of the canal at the Old Hammond Highway Bridge is discussed in this section. Cases 1 and 2 were tested with no debris blockage, whereas a 50% blockage at the bridge was included in Case 3. In Case 1, toe dumping was utilized for closure by using 31.1 kN (7,000 lb) sandbags. Toe dumping started from both sides of the channel upstream of the bridge together with

transverse dumping to form a stable weir until the channel was fully closed (Fig. 4.6). A similar scenario of sandbag dumping was followed in Case 2 and no significant differences between the two cases were observed. For Case 3, debris was already blocking about 50% of the flow area under the bridge. In this case the canal could be closed easily by using 31.1 kN (7,000 lb) sandbags without adopting any specific strategy (e.g., end toe or transverse dumping).



**Fig. 4.6.** Closure at Hammond Highway Bridge by using a combination of toe and transverse dumping for Cases 1 and 2 (looking south)

## **Discussion**

From these results, it can be concluded that the sandbags are a viable option for closing the 17th Street Canal breach in all cases tested for a maximum differential head of 1.67 m (5.5 ft) across the breach except in Case 1 using MBT2, which required an impractical sandbag size of 133.2 kN (30,000 lb) that is beyond the carrying capacity of available helicopters. Although it is not practical to place sandbags for breach closure by helicopters during a hurricane, it was assumed in this case study that the sandbags would be placed within a very short period after the storm peak. For Katrina, this would correspond to the late morning of August 29th, 2005, which

is Case 1 in these investigations. Table 4.3 lists the required number and size of sandbags for various cases (ranging from an average of 800 bags for closure at the bridge and 900 bags for closure at the breach). This should give an estimate of the time required to close the breach completely.

**Table 4.3.** Number and weights of sandbags used for closure at breach and at bridge

Case		Closure at breach		Closure at bridge	
		Number of sandbags	Weight [kN (lb)]	Number of sandbags	Weight [kN (lb)]
1	MBT1–Trial 1	410	31.1 (7,000)	800	31.1 (7,000)
		+460	44.4 (10,000)		
	MBT1–Trial 2	1,250	31.1 (7,000)		
	MBT2	275	44.4 (10,000)		
		+185	66.6 (15,000)		
+68	133.2 (30,000)				
2	MBT1	820	31.1 (7,000)	800	31.1 (7,000)
	MBT2	935	31.1 (7,000)		
3		590	31.1 (7,000)	380	31.1 (7,000)

## Chapter 5

### Velocity Profiles in Katrina Model

In this chapter velocity profiles at different locations in the Katrina model are presented. A movable grid was constructed over the studied area of the model. Fig. 5.1 shows the movable grid placed on the left half of the model and Fig. 5.2 shows the notation for the grid points in both the horizontal and vertical directions. In the horizontal direction, the notations are  $x_0, x_1 \dots x_{36}$ , while in the vertical direction the notations are  $y_0, y_1 \dots y_{25}$ . The vertical grid  $y_0, y_{8.5}, y_9,$  and  $y_{25}$  are spaced 7.62 cm (3 in) while the rest of the grid is spaced at 15.24 cm (6 in). The Acoustic Doppler Velocimeter (ADV) discussed before is used to measure the velocity at each grid points. Two cases were considered here, the first case with a model flow rate of 900 gpm and the second case with 1500 gpm.

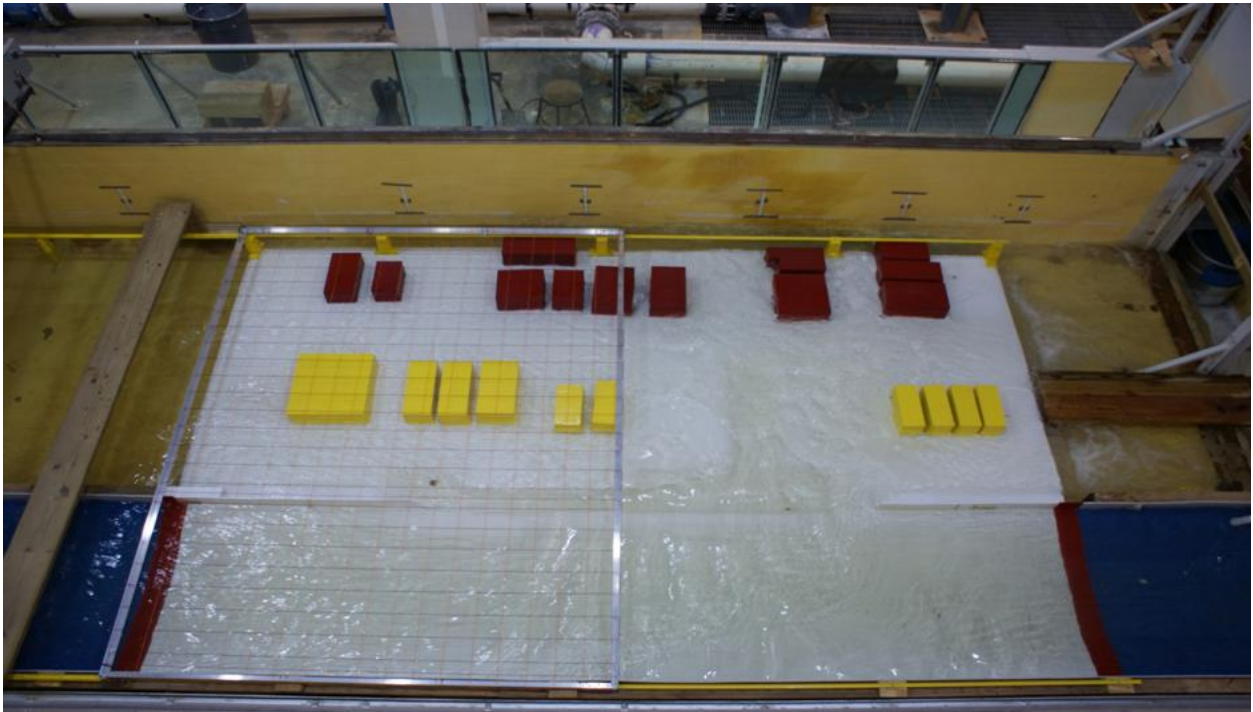


**Fig. 5.1.** A movable grid covering the left side of Katrina model

It should be mentioned that at some grid points especially on the crest of the breach and between the houses, the water depth was not sufficient to measure the flow velocity by ADV.

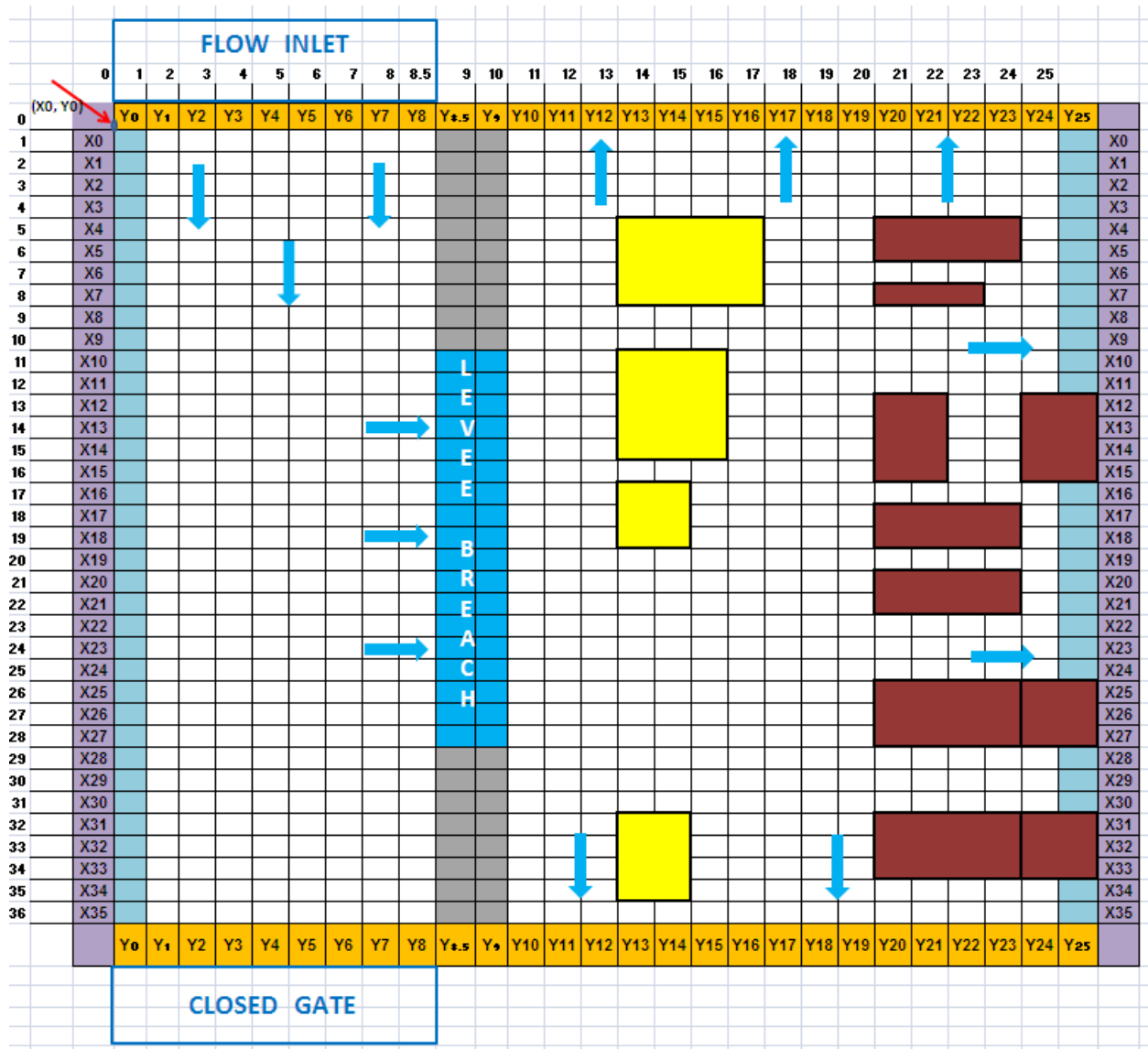


**Fig. 5.2.** Notations for all the grid points in the model

The elevation of the dry bed and the flow depths at all the grid points were measured by a point gauge with an accuracy of 0.1 mm. The flow depths for a flow of 900 gpm in the model is shown in Fig. 5.3. The maximum recorded flow depth was 18 cm in the entrance channel before the breach. In Fig. 5.4 a, b, c, d and e, the velocity profiles in the x and y directions are shown for selected grid points for a flow of 900 gpm. In Fig. 5.5a, b, c, d and e, the velocity profiles in the x and y directions are shown for selected grid points for a flow of 1500 gpm.

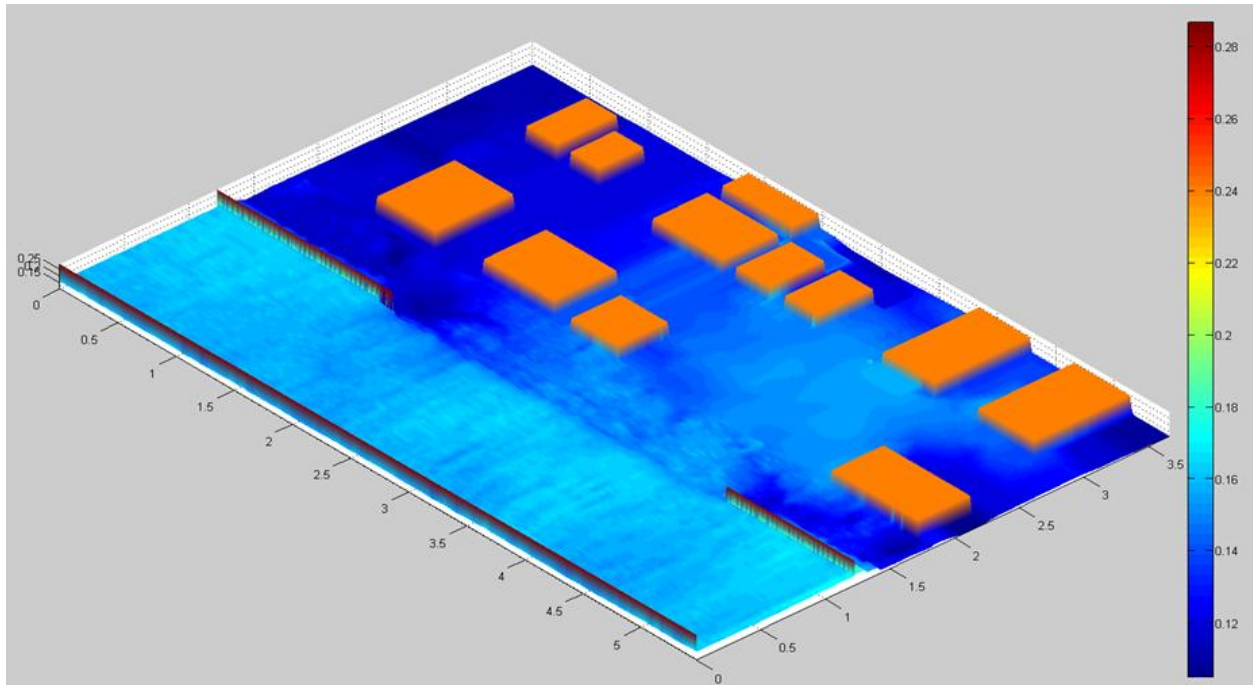
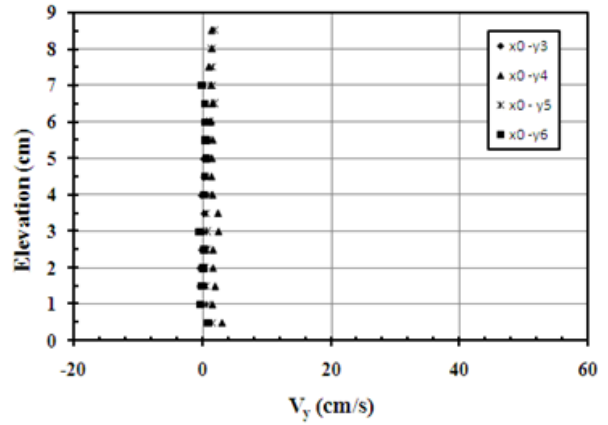
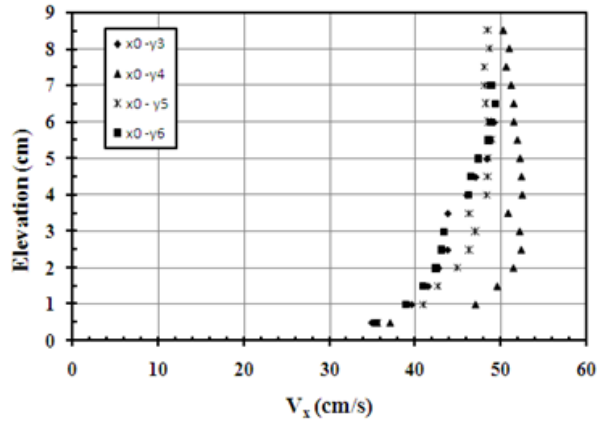


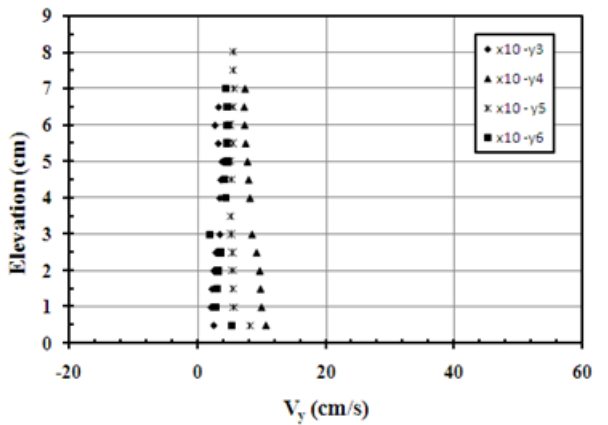
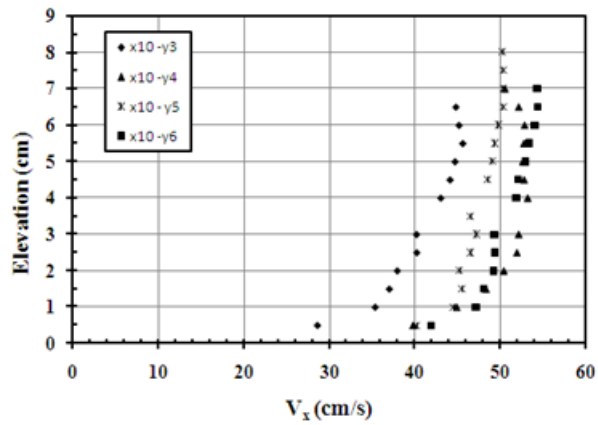
**Fig. 5.3.** Elevation of flow depths for a flow of 900 gpm in the model

## Results

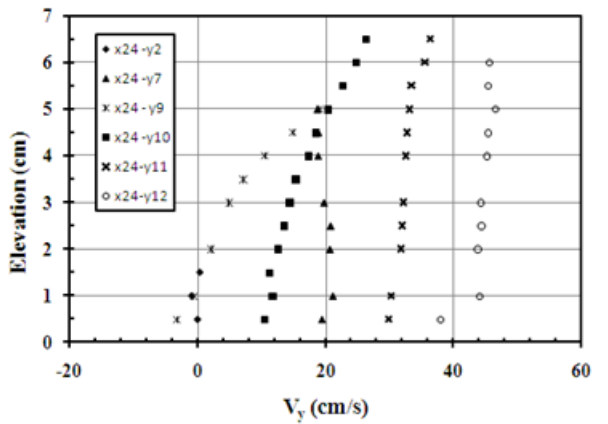
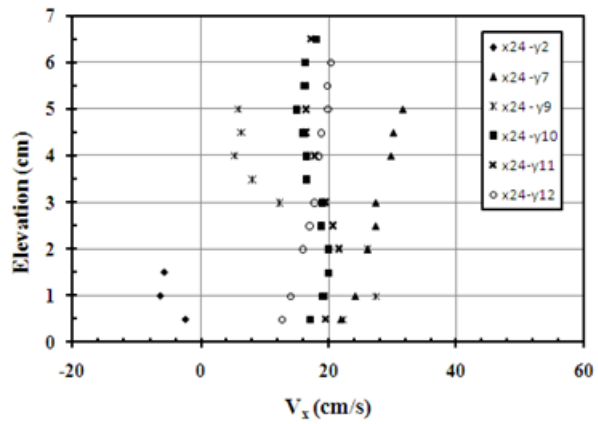
It may be noted by comparing the velocity profiles for 900 gpm that the velocity in x-direction is dominating until grid 'x10' where the velocity in y-direction starts to have some value. From Fig. 5.2, this grid is representing the end of the upstream levee and the beginning of the breach. At grid 'x24', the velocity in the y-direction is dominating while the velocity in the x-direction becomes almost zero. It should be mentioned also that because of the eddies and disturbances, the velocity profiles deviate from the shape of the well-known logarithmic profile, especially at the breach location. From the figures, the conclusions for the flow of 900 gpm is similar to that for 1500 gpm.



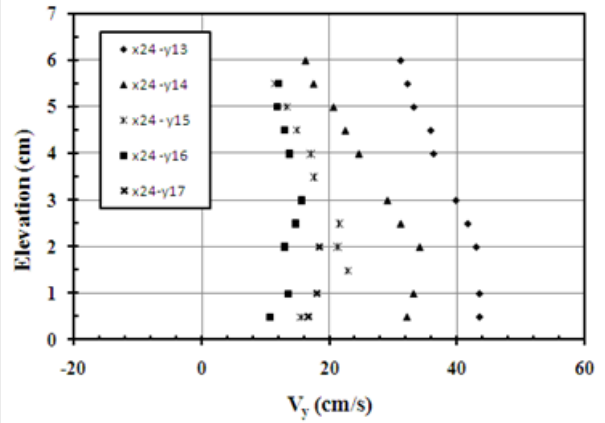
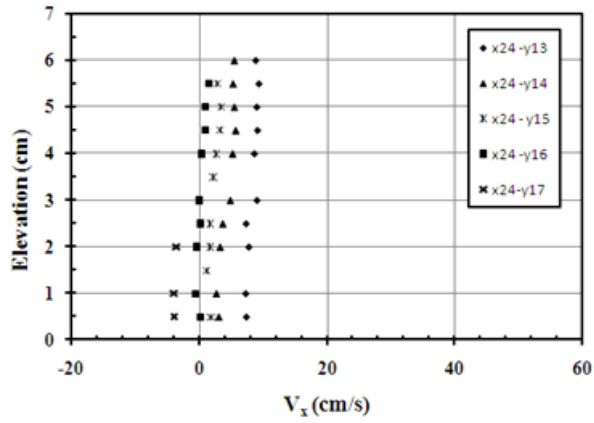
(a)



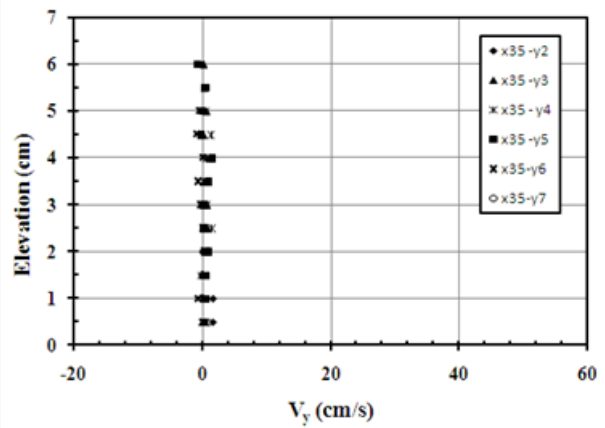
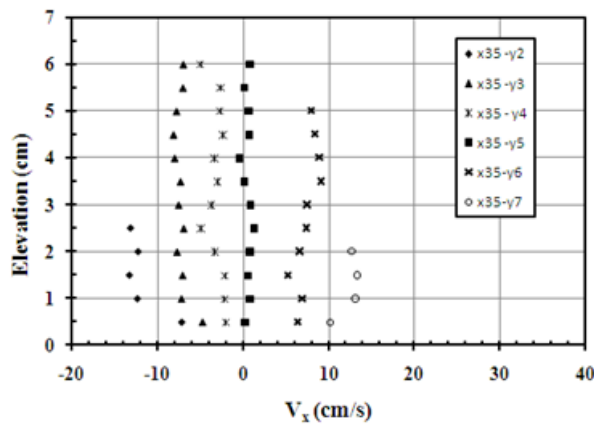
(b)



(c)

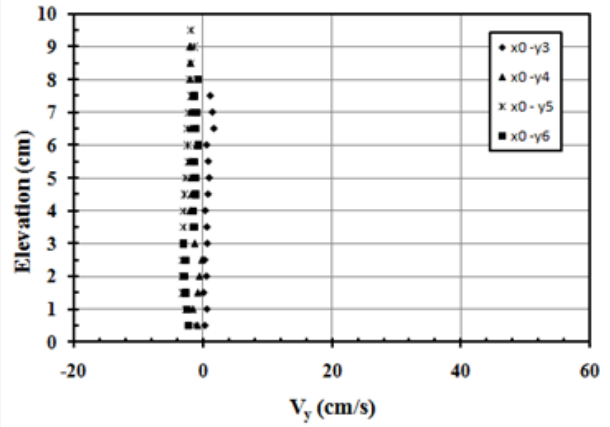
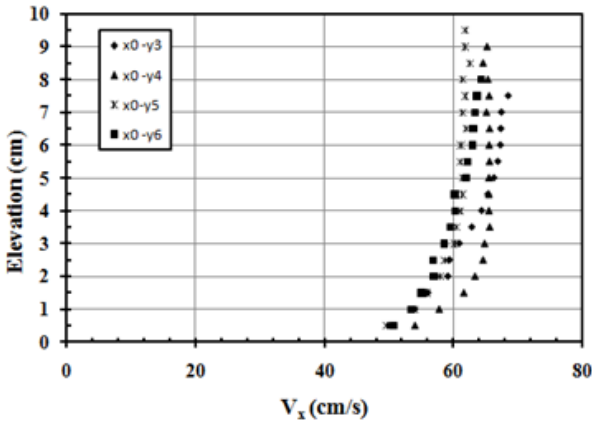


(d)

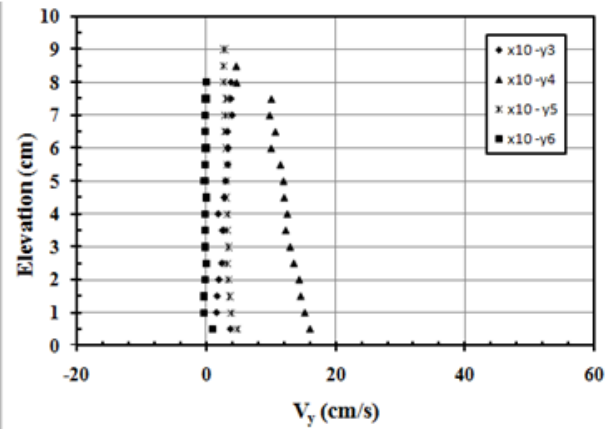
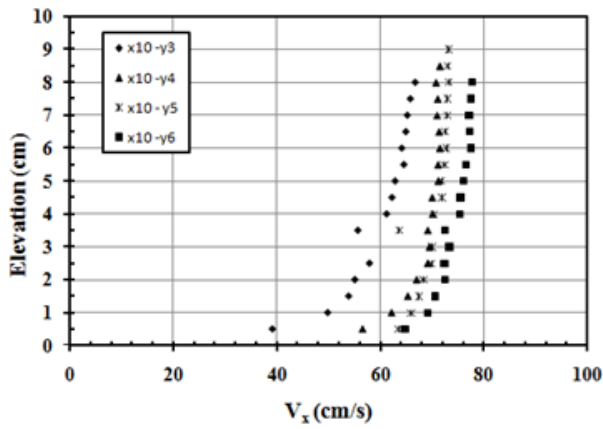


(e)

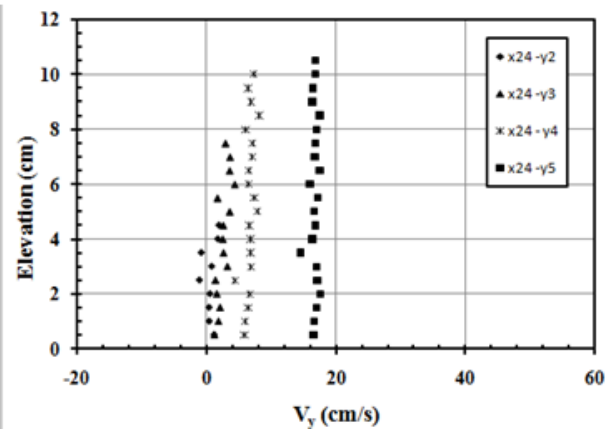
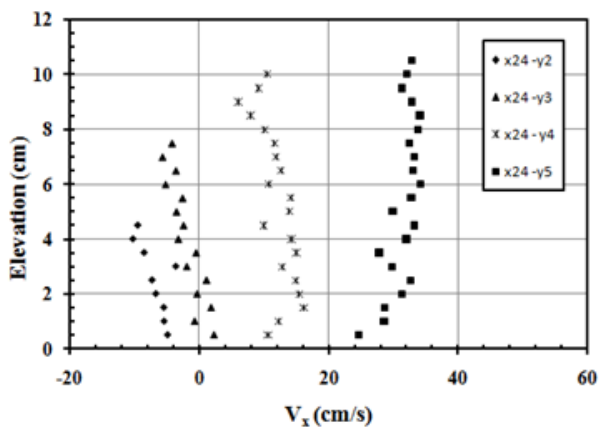
**Fig. 5.4.** Velocity profiles for 900 gpm at different x-grid (a) x0 - y3 to y6, (b) x10 - y3 to y6, (c) x24 - y2 to y12, (d) x24 - y13 to y17, (e) x35 - y2 to y7



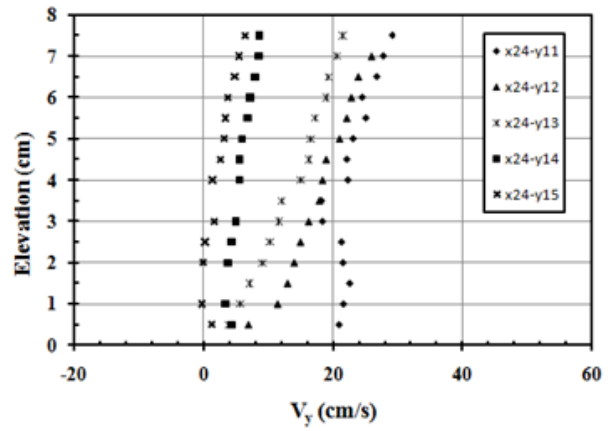
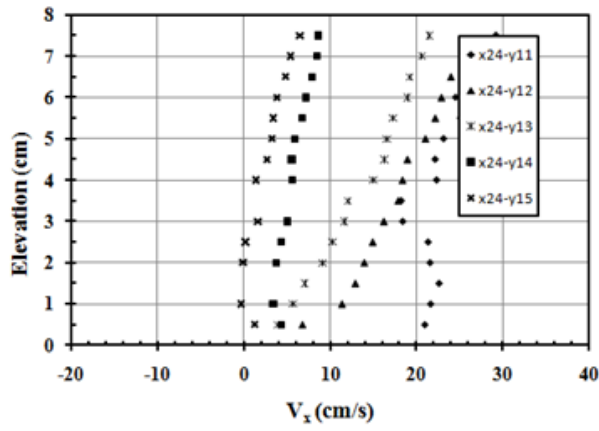
(a)



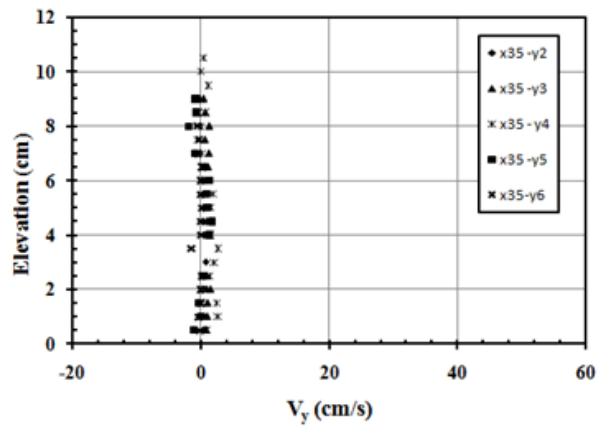
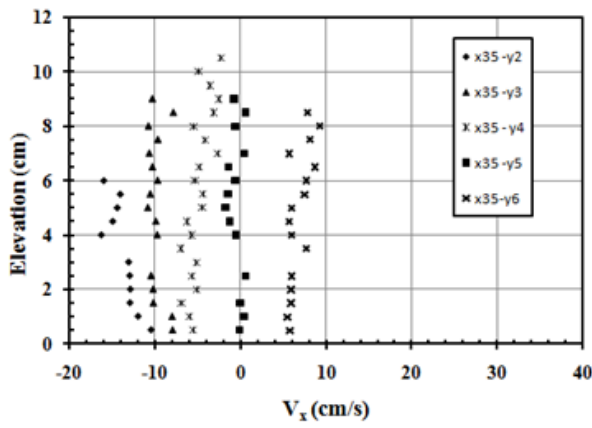
(b)



(c)



(d)



(e)

**Fig. 5.5.** Velocity profiles for 1500 gpm at different x-grid (a) x0 - y3 to y6, (b) x10 - y3 to y6, (c) x24 - y2 to y5, (d) x24 - y11 to y15, (e) x35 - y2 to y6

## Summary and Conclusions

A 1:50 scale physical model was constructed to simulate the 17<sup>th</sup> Street Canal levee breach and the flooded neighborhood in the hydraulic laboratory at the University of South Carolina. The physical model has been validated against available data in the IPET report. Tests for the stability of sandbags at different locations along the breach showed that, for water elevation in the channel of 9 ft, sandbags weighting 30,000 Ib and 50,000 Ib would be required to close the breach and that the 6,000 Ib sandbags used by the USACE would be easily washed away. The results also show that the Digital Particle Tracking Velocimetry technique is capable to develop the trajectories of the sandbags both in plan view and in the vertical direction. This provide information for the particles motion and leads to a more comprehensive study to estimate the size of the dumped materials that can resist the water force under flood flow conditions. The experiments for the threshold of motion in this study are highly reliable for the observation of general trends presented earlier by different researchers. Reasonable agreement is achieved in comparing the laboratory results with the field results replaced by other investigators. The results show that various closure procedures for cofferdam closure, e.g., transverse dumping, toe dumping and multi-dike system, could have been used for the closure of the 17<sup>th</sup> Street canal breach using lighter sandbags. These closure procedures divided the total head at the breach, thus reducing the flow velocity through the breach. These investigations are based on the best estimated values by the USACE (2007) for various variables, such as different water levels in the channel and the degree of blockage at the Old Hammond Highway Bridge.

Although the results presented herein confirm the viability of the use of sandbags with these types of multi-barriers to effectively close the 17th Street Canal breach, care must be exercised in extending these results to other breaches in which levees and the channel bottom may erode during closure and the differential heads across the breach may be higher. Similar hydraulic model with movable bed and erodible levee sections at breach locations may be used to investigate such cases.

## References

- Abacasis, M., Quintela, C., Henriques, G., and Santos, M. “Temporary river diversion. The case of Cabora Bassa.” *Trans., International commission of Large Dams*, vol. II, Madrid, pp. 815-831, 1973.
- Adrian, R. J. “Particle-imaging Techniques for Experimental Fluid Mechanics.” *Ann Rev Fluid Mech*, 23, pp. 261-304, 1991.
- Aguirre-Pe, J., Olivero, M.L., Moncada, A.T. “Particle densimetric froude number for estimating sediment transport”, *J. Hydr. Eng.*, vol. 129, no. 6, pp. 428-437, 2003.
- Arroyo, M. P., Greated, C. A. “Stereoscopic Particle Image Velocimetry.” *Meas Sci Technol*, vol. 2, pp. 1181-1186, 1991.
- Buffington, J.M. “The legend of A. F. Shields”, *J. Hydr. Eng.*, vol. 125, no. 4, pp. 376-387, 1999.
- Chanson, H. “*The hydraulics of open channel flow*”, Arnold, London, 1999.
- Cortim, J., Krauch, H., Rocha, J., Gallico, A., and Sarkaria, G. “The bi-national Itaipu hydropower project.” *Int. Water Power Dam Constr.*, vol. 29, pp. 40–47, 1977.
- Defne, Z. “Effect of particle shape and size on incipient motion of solid particles”, MS thesis, Middle East Technical Univ., Ankara, Turkey, 2002.
- El-Kholy M., Chaudhry, M. H. “Tracking Sandbags Motion during Levee Breach Closure using DPTV Technique”, *33rd Congress, International Association of Hydraulic Engineering and Research*, Aug. 2009.
- El-Kholy, M. and Chaudhry, M. H., “Incipient Motion of Large Sandbags in a fixed Bed Channel,” *Jour. Hydraulic Engineering*, (Under revision).

- Goguş, M., Defne, Z. “Effect of shape on incipient motion of large solitary particles’,  
*J. Hydr. Eng.*, vol. 131, no. 1, pp. 38-45, 2003.
- Goldman, D. “Estimating expected annual damage for levee retrofits.” *J. Hydr. Eng.*,  
vol. 123, no. 2, pp. 89–94, 1997.
- Gui, S., Renduo, Z., and Xue, X. “Overtopping reliability models for river levee.” *J.  
Hydr. Eng.*, vol. 124, no. 12, pp. 1227–1234, 1998.
- Hassan, Y. “Full-Volume, 3-D Transient Measurements of Bubbly Flows Using PTV and  
Shadow Image Velocimetry Coupled with Pattern Recognition Techniques.” *Final  
Report, DOE Project DE-FG07-98ID13638, Department of nuclear Engineering, Texas  
A&M University*, 2001.
- Henderson, F. M. “Open channel Flow”, Macmillan, 1966.
- Jaffe, D., and Sanders, B. “Engineered levee breaches for flood mitigation.” *J. Hydr.  
Eng.*, vol. 127, no. 6, pp. 471–479, 2001.
- Kramer, H. “Sand mixtures and sand movement in fluvial models”, *Trans. Am. Soc.  
Civ. Eng.*, vol. 100, pp. 798-878, 1935.
- Lavelle, J. W., and Mofjeld, H. O. “Do critical stresses for incipient motion and  
erosion really exist?”, *J. Hydr. Eng.*, vol. 113, pp. 370-385, 1987.
- Lecerf, A., Renou, B., Allano, D., Boukhalfa, A., Trinite, M. “Stereoscopic PIV:  
Validation and Application to an Isotropic Turbulent Flow.” *Exp Fluids*, vol. 26, pp. 107-  
115, 1999.
- Loth, E. “Drag of non-spherical solid particles of regular and irregular shape”,  
*Powder Technology*, vol. 182, pp.342-353, 2008.

- Maas, H. G., Gruen, A., Papantoniou, D. “Particle Tracking Velocimetry in Three-Dimensional Turbulent Flows.” Part 1: The Imaging Technique. *Exp Fluids*, vol. 15, pp. 133-46, 1993.
- Novak, P., Nalluri, C. “Incipient motion of sediment particles over fixed beds”, *J. Hydr. Eng.*, vol. 22, no. 3, pp. 181-197, 1984.
- Parmley, L. “Seven mile hydroelectric project: Hydraulic design of diversion facilities”  
*Presented at Meeting of the Canadian Electrical Association, Toronto, 1978.*
- Prasad, A. K., Adrian, R. J. “Stereoscopic Particle Image Velocimetry Applied to Liquid Flows.” *Exp Fluids*, vol. 15, pp. 49-60, 1993a.
- Shields, A. “Application of similarity principles and turbulence research to bedload movement (English translation of the original german manuscript)”, Hydrodynamics Laboratory, California Institute of Technology, Publication No. 167, 1936.
- SonTek/YSI, “ADV operation manual, version 7.9”, Available from sonTek/YSI, Inc., 6837 Nancy Ridge Drive, Suite A, San Diego, CA 92121-3217, 2001.
- Sattar, A.M., Kassem, A.M., Chaudhry, M.H. “Case Study: 17th Street Canal Breach Closure Procedures”, *J. Hydr. Eng.*, ASCE, vol. 134, pp.1547–1558, 2008.
- Soloff, S. M., Adrian, R. J., Liu, Z. C. “Distortion Compensation for Generalized Stereoscopic Particle Image Velocimetry.” *Meas Sci Technol*, vol. 8, pp. 1441-1454, 1997.
- Thomas, A., and Gwyther, J. “Diversion of River Jhelum during construction of Mangla Dam.” *Transactions 9th International Congress on Large Dams ICOLD*, Istanbul, 1967.
- United States Army Corps of Engineers (USACE) “Interagency performance

- evaluation taskforce (IPET)” *Final Rep.*, March, June 2007, ([www.ipet.wes.army.mil](http://www.ipet.wes.army.mil)).
- Vanoni, V.A. “Sedimentation Engineering”, ASCE Task Committee for the preparation of the Manual on Sedimentation of the Sedimentation Committee of the Hydraulics Division (reprinted 1977).
- Xu, G., Zhang, L., and Liu, S. “Preliminary study of instability behavior of levee on soft ground during sudden drawdown.” *Part of Geo-Frontiers 2005 ASCE Conf., Austin, Texas, USA*, vol. 166, pp. 130– 142, 2005.
- Ying, X., Wang, S., and Khan, A. “Numerical simulation of flood inundation due to dam and levee breach.” *Proc., World Water & Environmental Resources Congress 2003*, P. Bizier and P. DeBarry, eds., ASCE, Philadelphia.
- Zhu, L., Wang, J., Cheng, N.S., Ying, Q., Zhang, D. “Settling distance and incipient motion of sandbags in open channel flows”, *J. Hydr. Eng.*, ASCE, vol. 130, pp.98-103, 2004.